PISCES Research Program 2020 Highlights & Future Directions

Matt Baldwin* & *PISCES team
(UC-San Diego)

UCSD CENTER FOR ENERGY RESEARCH

2020 Research highlights.

- Study of D retention in Be-D co-deposits in varied neutral pressure enviroments.
- Study of D retention in Be-W co-deposited layers.
- Simulated strike point sweeping D removal from Be-D co-deposited layers.
- D retention in RAFM steels.
- In-situ diagnostic development: LIBS & HIS experiments.
- ERO 2.0 validation of PISCES-B Be erosion.
- PISCES – future direction.

D retention in Be-D co-deposits in varied neutral pressure environments above and below ~1 Pa.

Be-D co-deposits are produced in a programmable feedback-controlled Be coating system.

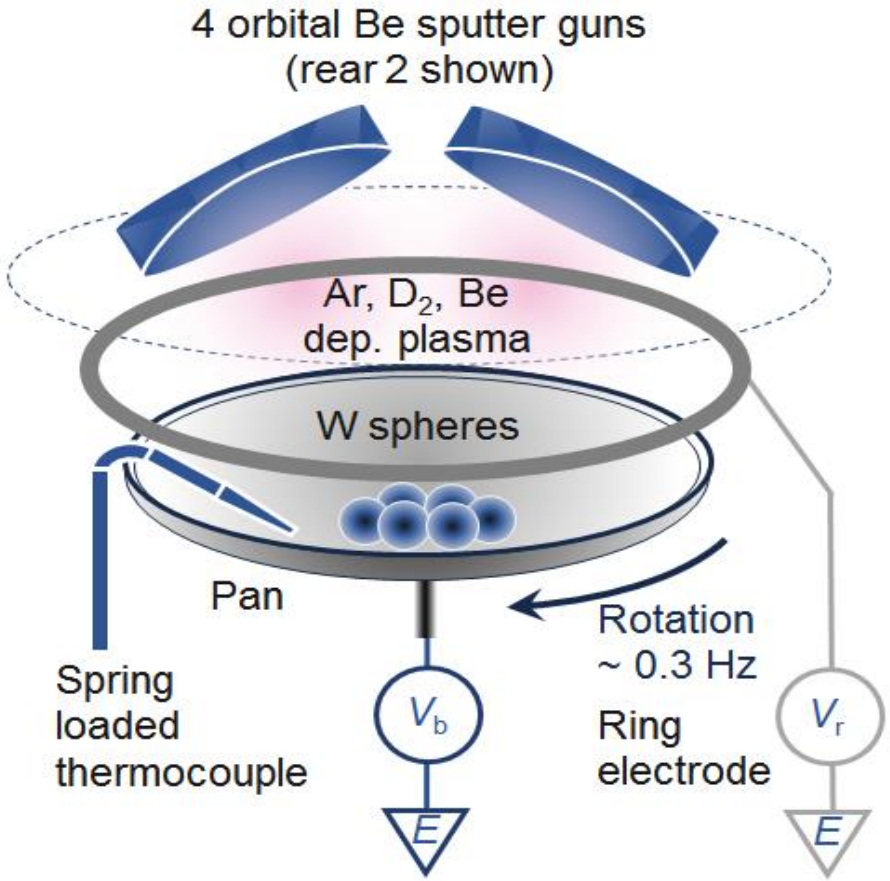

Be safety enclosure

chamber

monitor

TDS
station

labview
GUI & DAQ

UCSD Center for Energy Research

TDS Data collection / modeling

- TDS on Be-D up to 1273 K, β=0.3 K/s.
- We now also model TDS data with TESSIM.

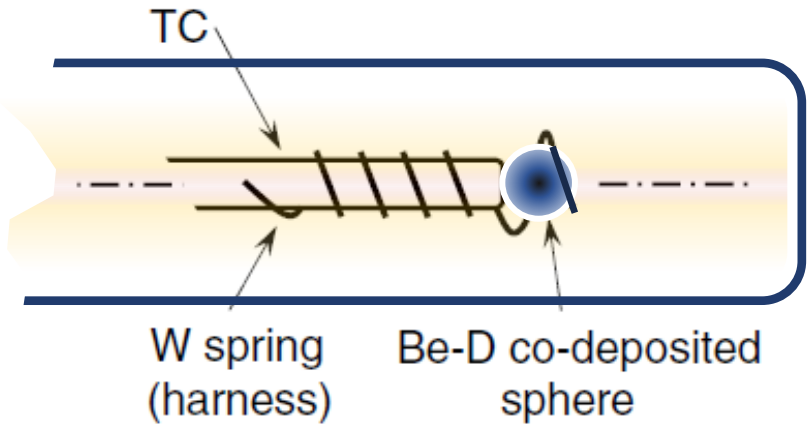

Properties				Ref.
Bulk-thermal (pure Be)				
Conductivity	κ	($W\,m^{-1}\,K^{-1}$)	168	[33]
Density	ρ	($kg\,m^{-3}$)	1848	[33]
Specific heat	C_p	($J\,kg^{-1}\,K^{-1}$)	1825	[33]
Transport (D in pure Be)			$A = A_0 e^{-E/kT}$	
Diffusivity	D_0	($m^2\,s^{-1}$)	8×10^{-9}	[8, 34]
	E_m	(eV)	−0.364	
Solubility	S_0	($m^{-3}\,Pa^{-1/2}$)	2.3×10^{22}	[8, 18]
	E_s	(eV)	−0.174	
D–D_2 surface	K_0	($m^4\,s^{-1}$)	3.4×10^{-29}	[19]
Recombination	E_r	(eV)	−0.280	

See Refs. in M.J. Baldwin *et al*. (2014) Nucl. Fusion **54** 073005

- Be co-deposit model has evolved over time.
  - Main parameters: retention mechanism concentrations & release energies.
  - TMAP & two traps – no sharp peak in data, occupancies as free parameters.
  - TMAP & three traps – thermal history included, trap occupancies not free parameters – some data could not be modeled due to sharp peak.
  - TESSIM – four traps and sharp peak now modeled.

T_0 desorption resembles M-MH_x de-composition.

- TDS data w/o T_0.

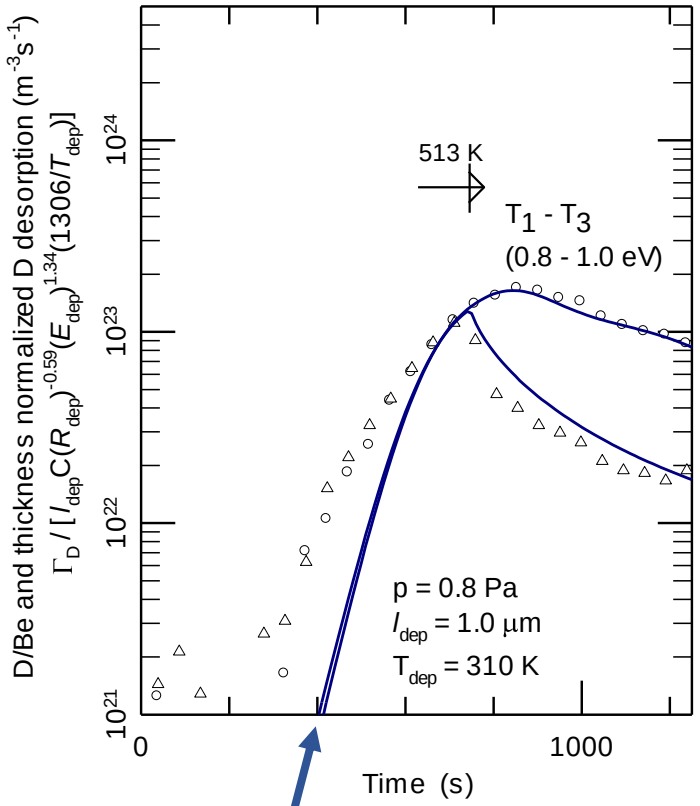

- TMAP trap physics can model ramp & ramp and hold TDS data when T_0 is absent.

- TMAP can not simulate sharpness of T_0.
- TMAP can not simulate 'flat' desorption.
- Constant *T*, 'flat' desorption implies fixed mobile D conc.
- M-MH_x decomp. chemistry is well known for this.

- TESSIM simulations with hydride physics included performed by *Anže Založnik.*
- Agreement with TDS data suggests T_0 is a decomposition signature for BeD_x. (Lines are TESSIM simulation)

- TDS data w/ T_0.

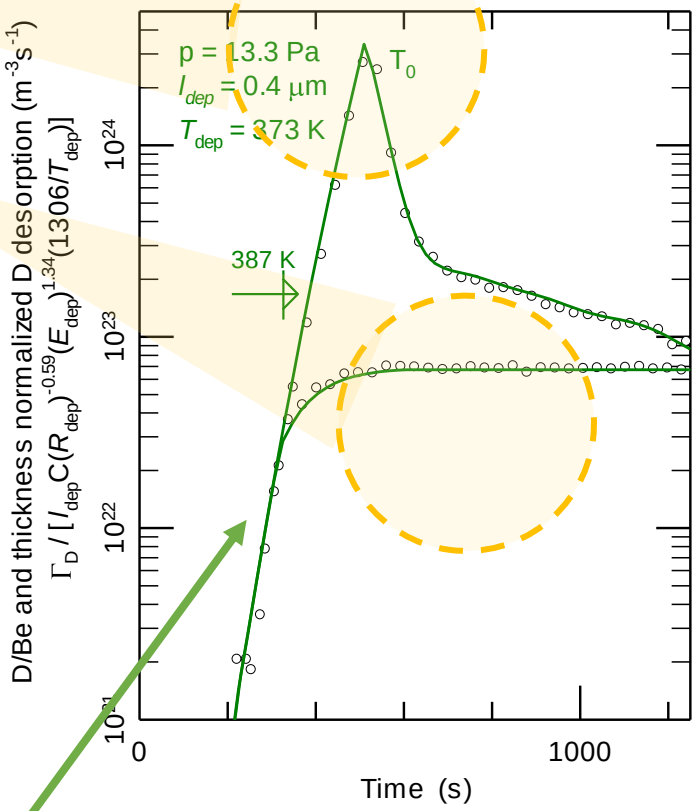

A. Založnik *et al* (2019) Modeling the sharp deuterium release from beryllium co-deposits, Nucl. Fusion **59** 126027

Recent experiments: A focus on pressure.

- Study relationship between co-deposit formation conditions and presence of the T_0 feature in TDS data for 1 h deposition runs.

p (Pa)	T_{dep} (K)	E_{dep} (K)	*Variation*
0.2 - 13	373	40	Pressure
2.67	373	20 - 200	Deposition energy, above 1 Pa
0.83	373	20 - 200	Deposition energy, below 1 Pa
0.2 - 13	373 - 610	20 - 200	Deposition temperature, (all data)

- Develop TESSIM models for all TDS data.
- Study the relationship between retention mechanisms relative to bake temperature.
- Simulate 1 & 10 h baking on co-deposits representative of each experiment.

Examining the new data.

- Co-deposits formed versus a range of PMI parameters.
- TDS data are then produced.
- TDS data are modelled with TESSIM
- Retention states are characterized by mechanisms $T_0 - T_4$.
- Concentrations in retention states are grouped relative to ITER bake temperatures T_{b1} (513 K) and T_{b2} (623 K).

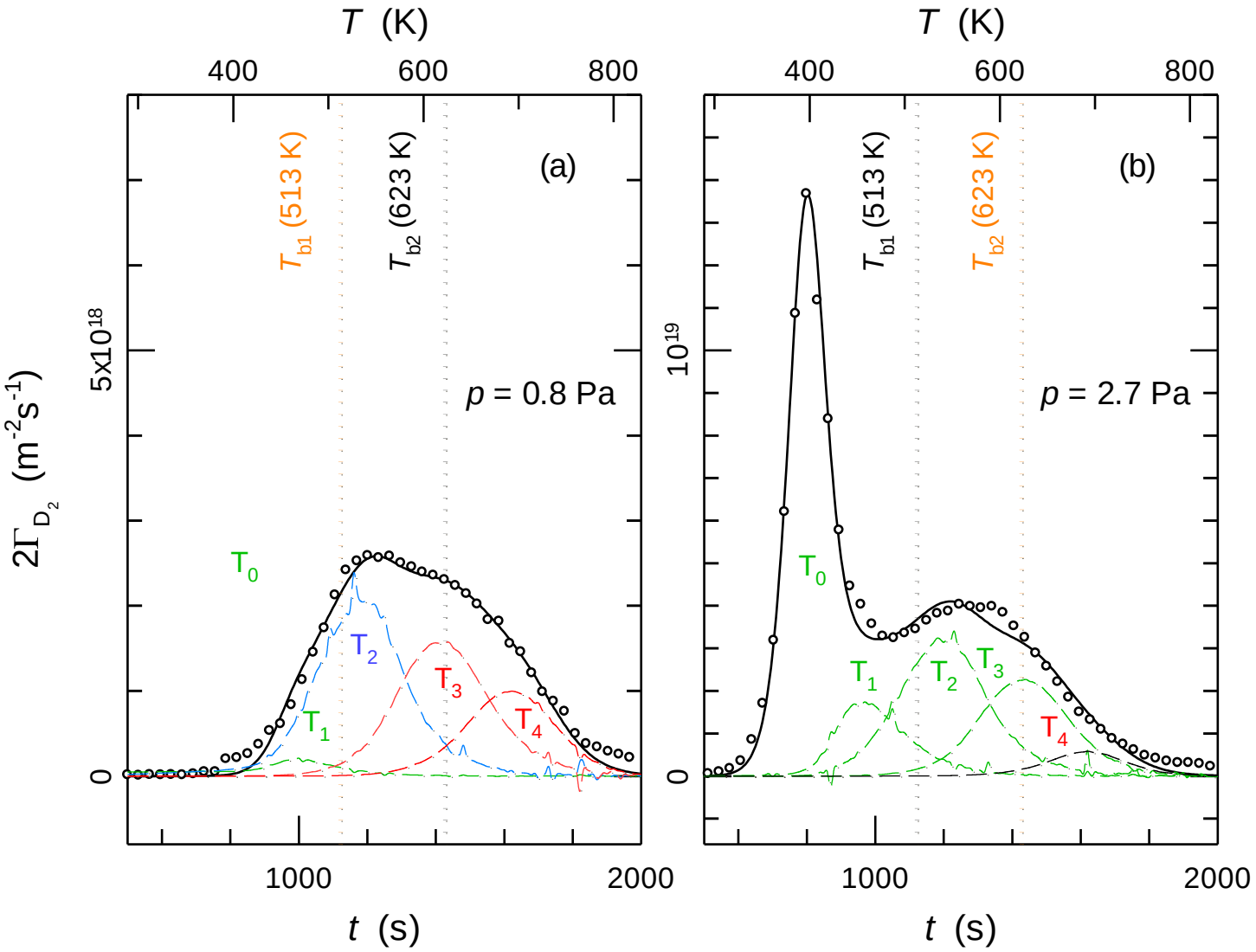

Increased *p*, gives more D in easily baked retention mechanisms.

T_{dep}=373 K, E_{dep} = 40 eV

As *p* increases:

- More D is trapped in low T mechanisms.
- Higher energy trapping is somewhat suppressed.

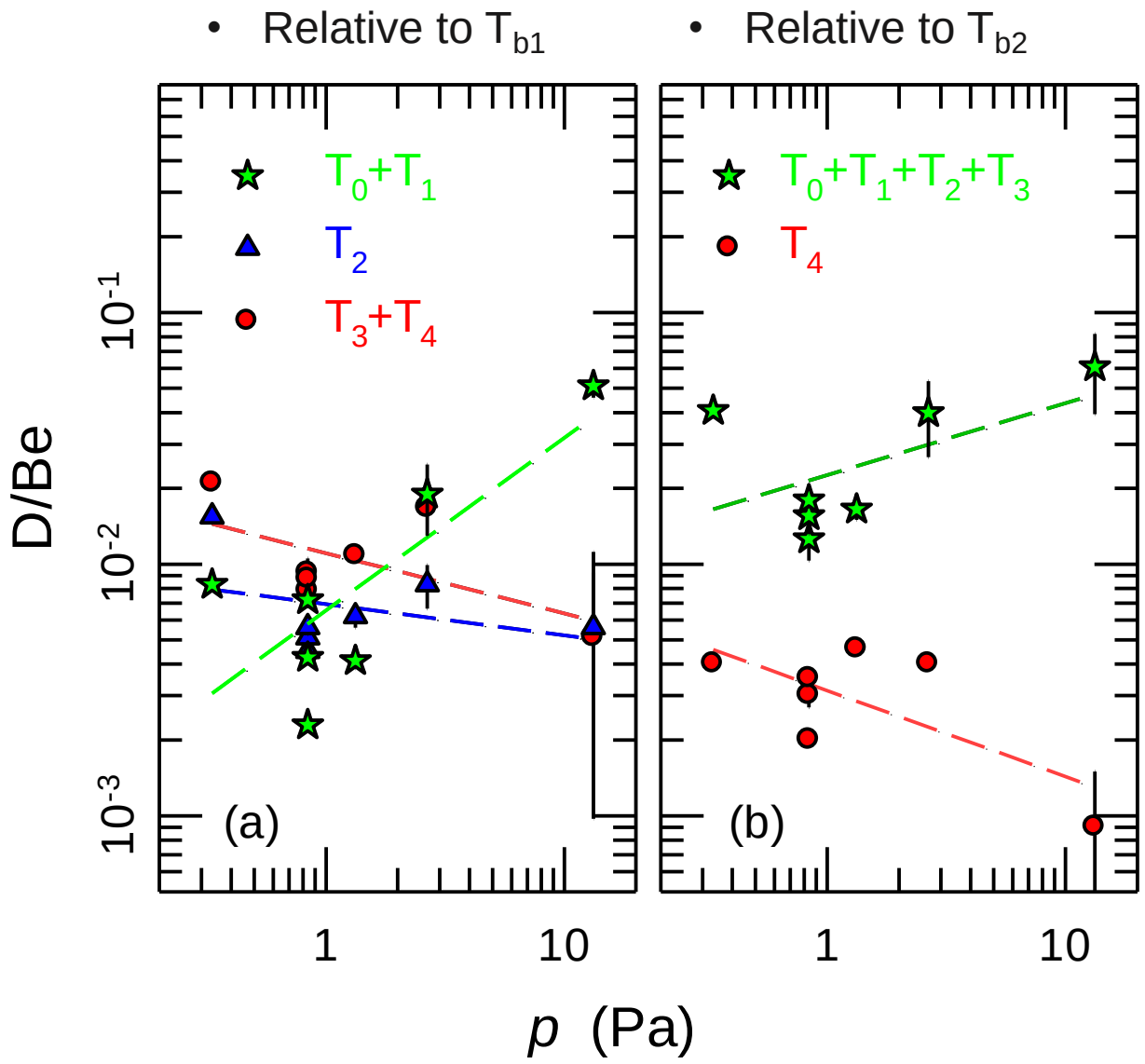

Increased E_{dep}, gives more D in easily baked retention mechanisms at higher *p*.

T_{dep}=373 K, p = 2.67 Pa

As E_{dep} increases:

- More D is trapped in low T mechanisms.
- Higher energy trapping seems little affected.

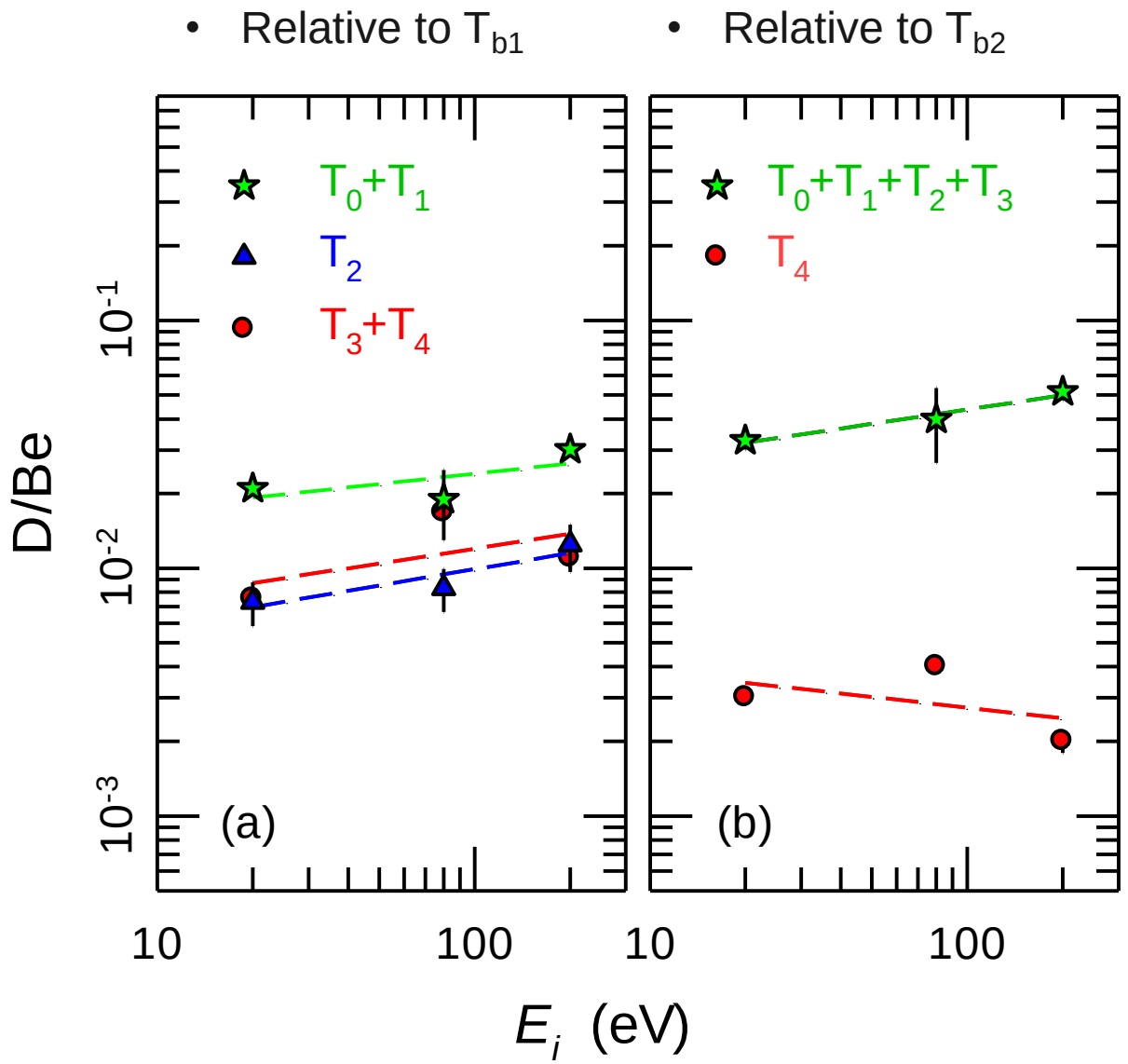

Increased E_{dep}, gives little change in retention groups at lower *p*.

T_{dep}=373 K, p = 0.8 Pa

As E_{dep} increases:

- Possible ‘small’ loss of bake efficacy at T_{b1}. due to falling trend in T_0+T_1.
- But not strongly seen in group $T_0+T_1+T_2+T_3$ relative to T_{b2}.

At lower p, no overly convincing energy dependence.

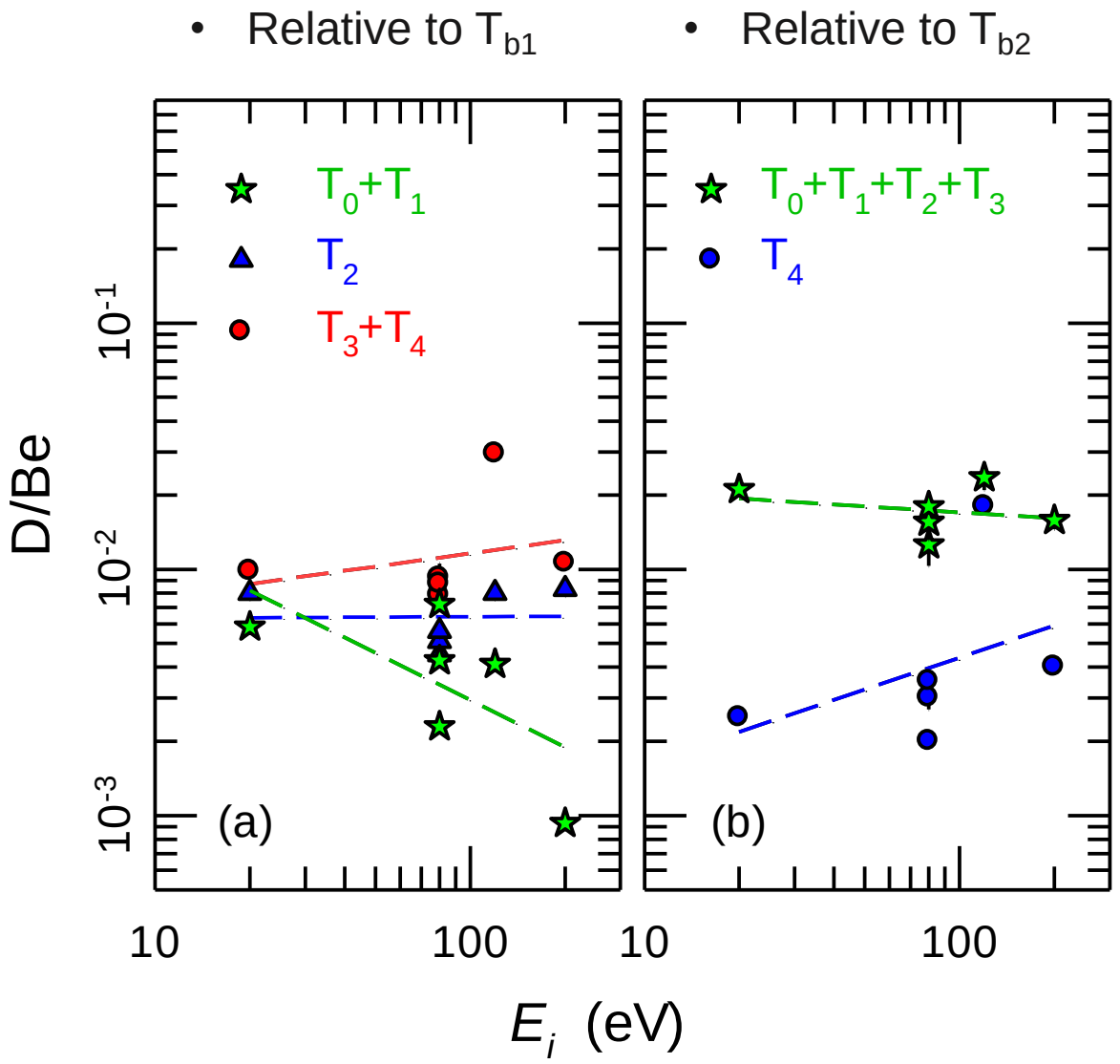

T_{dep} plot suggests retention mechanisms T_3+T_4 and T_4 may require removal means other than baking.

All data of study

As T_{dep} increases:

- Retention mechanisms T_3,T_4 persist at temperatures higher than the ITER bake temperatures.
- Target removal techniques (i.e. laser based methods, divertor strike point sweeping etc. may be necessary).

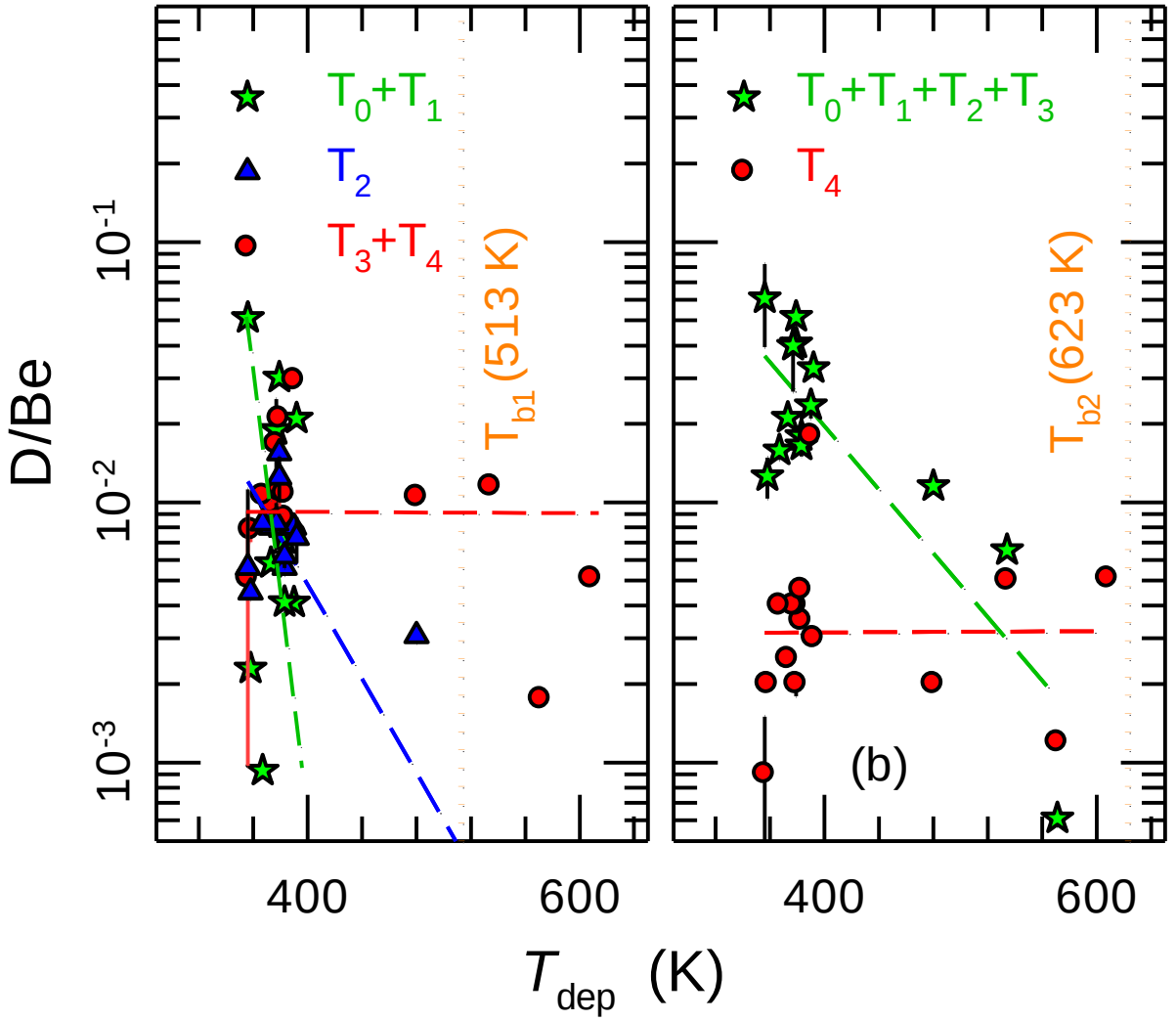

D retention in Be-W co-deposited layers.

Layer codeposition

- Substrates: 3 Mo and 1 Si
- Ar-D_2 mixture; D_2 fraction: ~15%

  p = 0.8, 2.7, 8.0 Pa
- 3 Beryllium guns at 100 W;

  1 Tungsten gun at 1–100 W
- T_{dep} = 373 ± 15 K

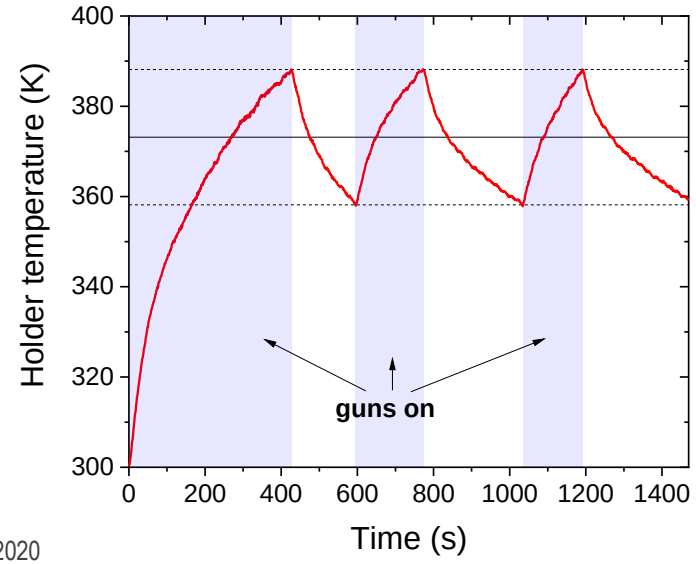

3 Be and 1 W confocal sputter guns

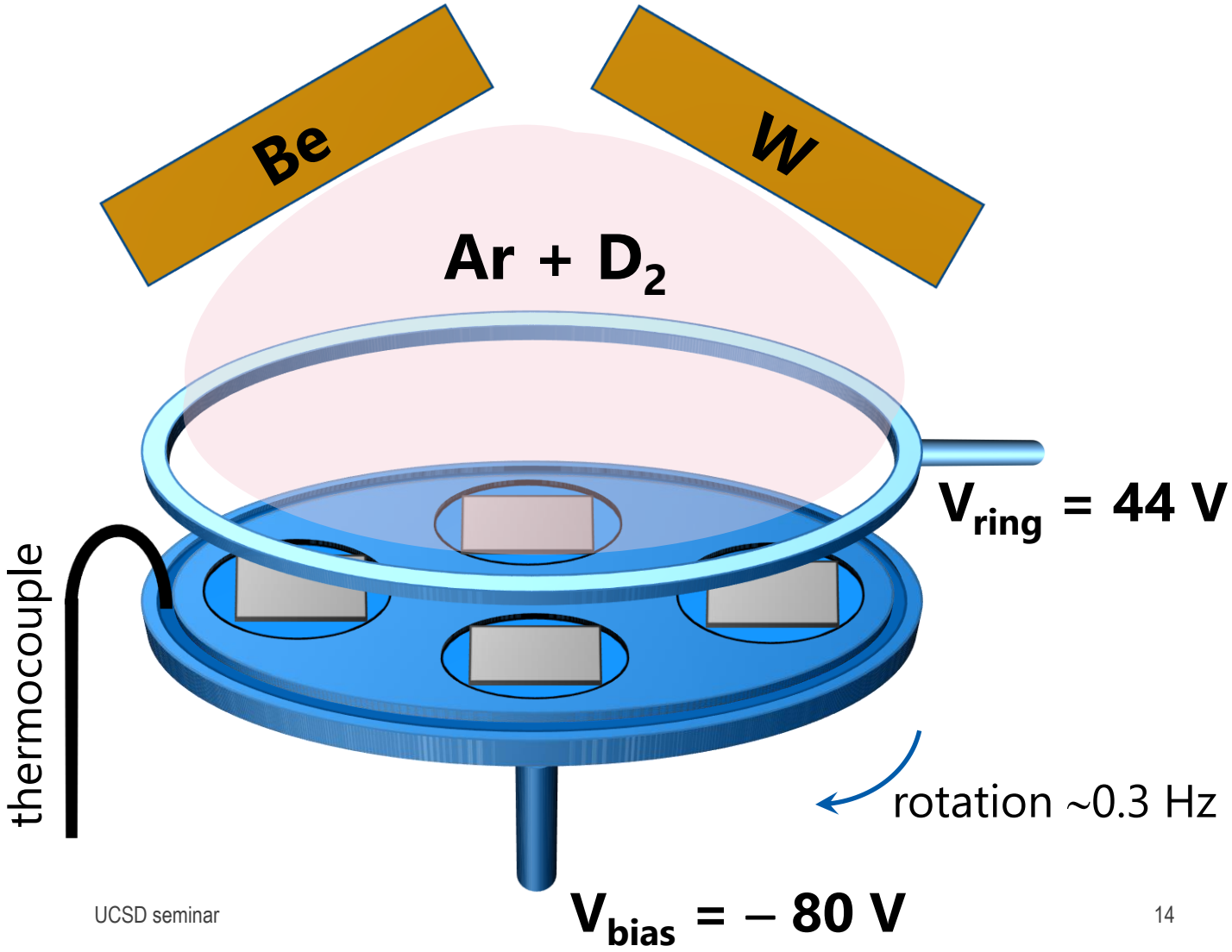

Layer composition: ion beam analysis

- ^{3}He ions: 1.2, 2.4, 4.5 MeV
- Rutherford backscattering spectrometry (RBS):
  → Areal density and W concentration

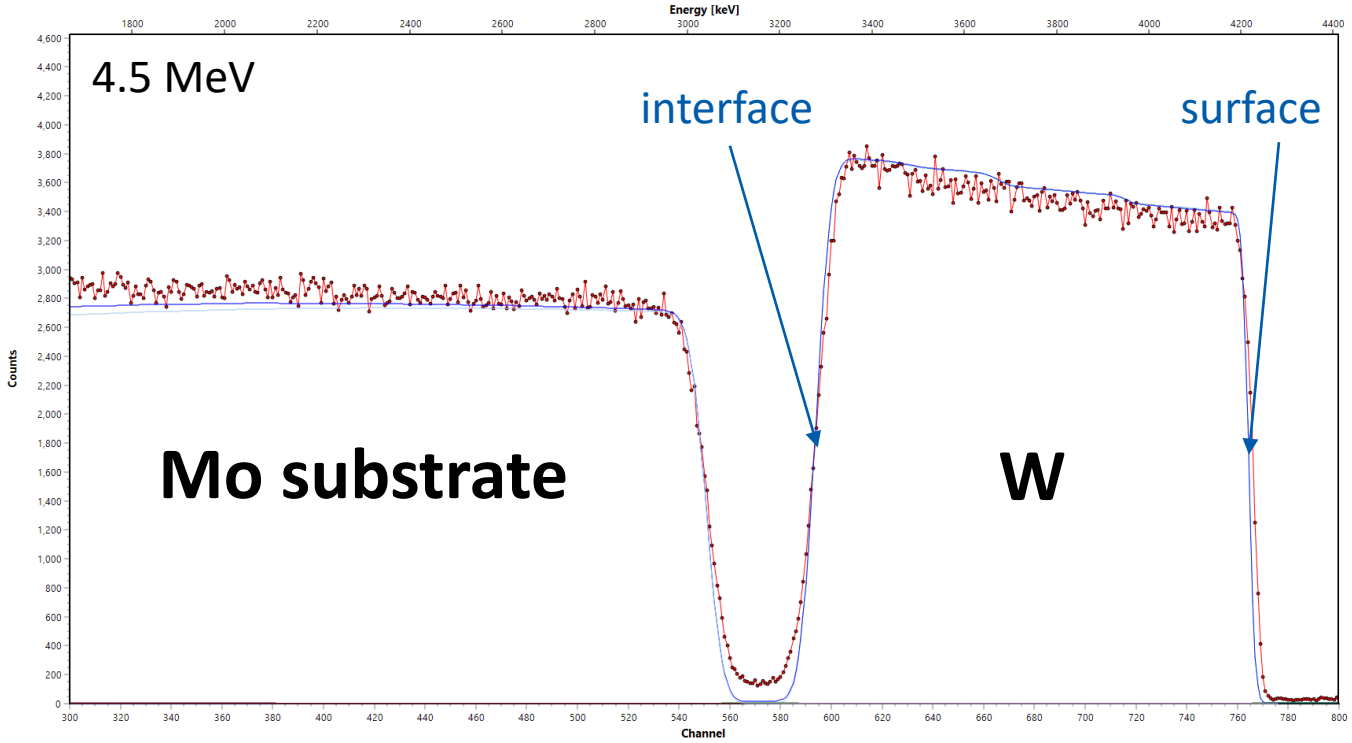

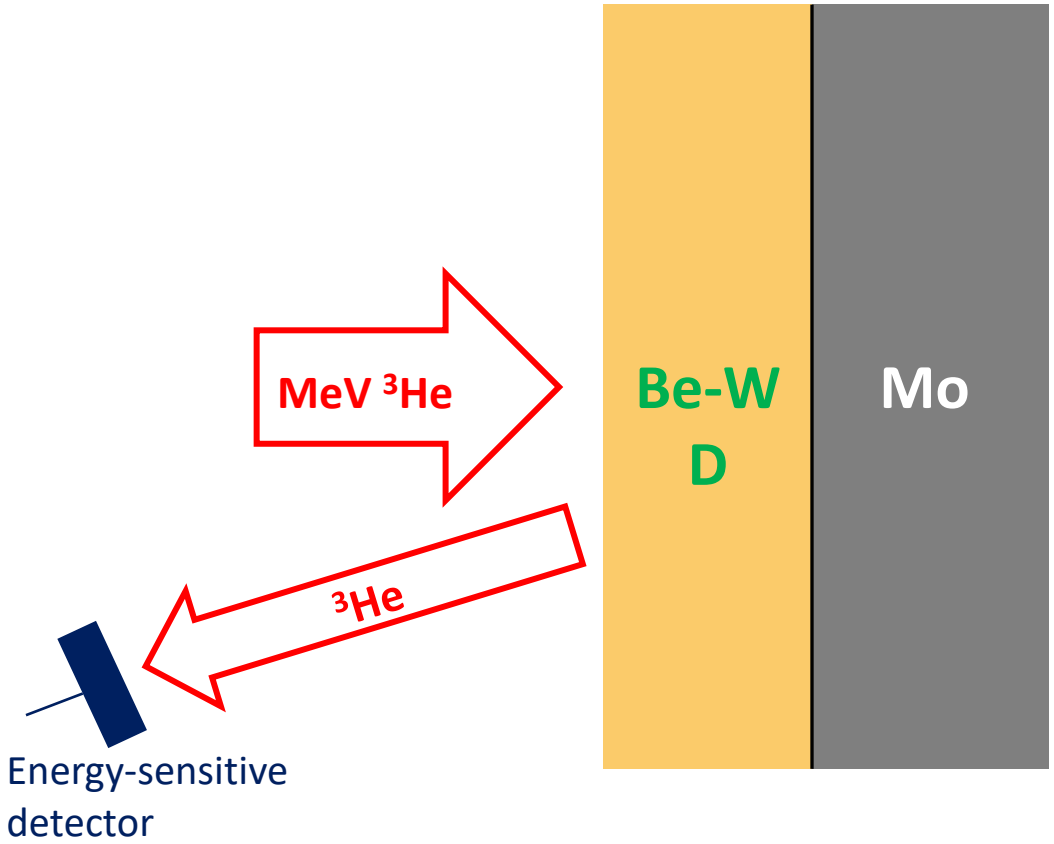

- Fitting of measured energy spectra in SIMNRA 7

Layer composition: ion beam analysis

- ^{3}He ions: 1.2, 2.4, 4.5 MeV
- Nuclear reaction analysis (NRA):
  → D concentration

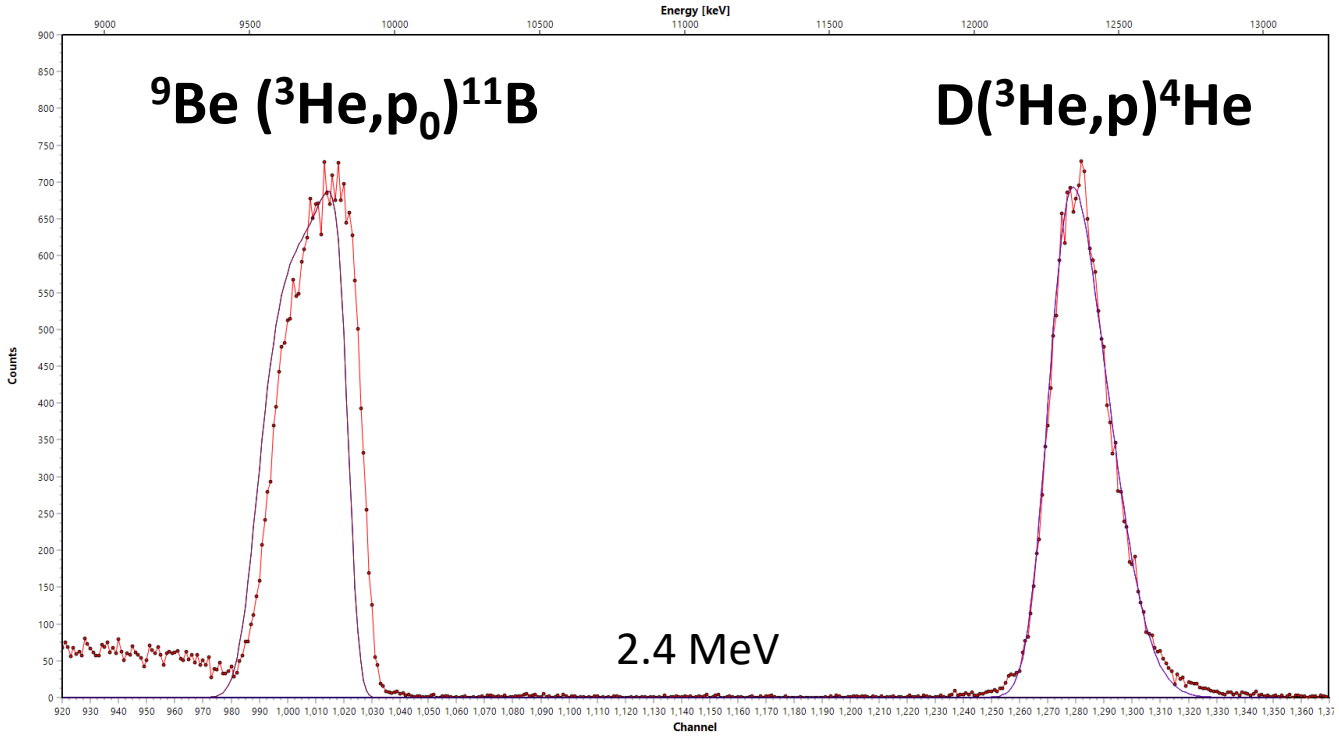

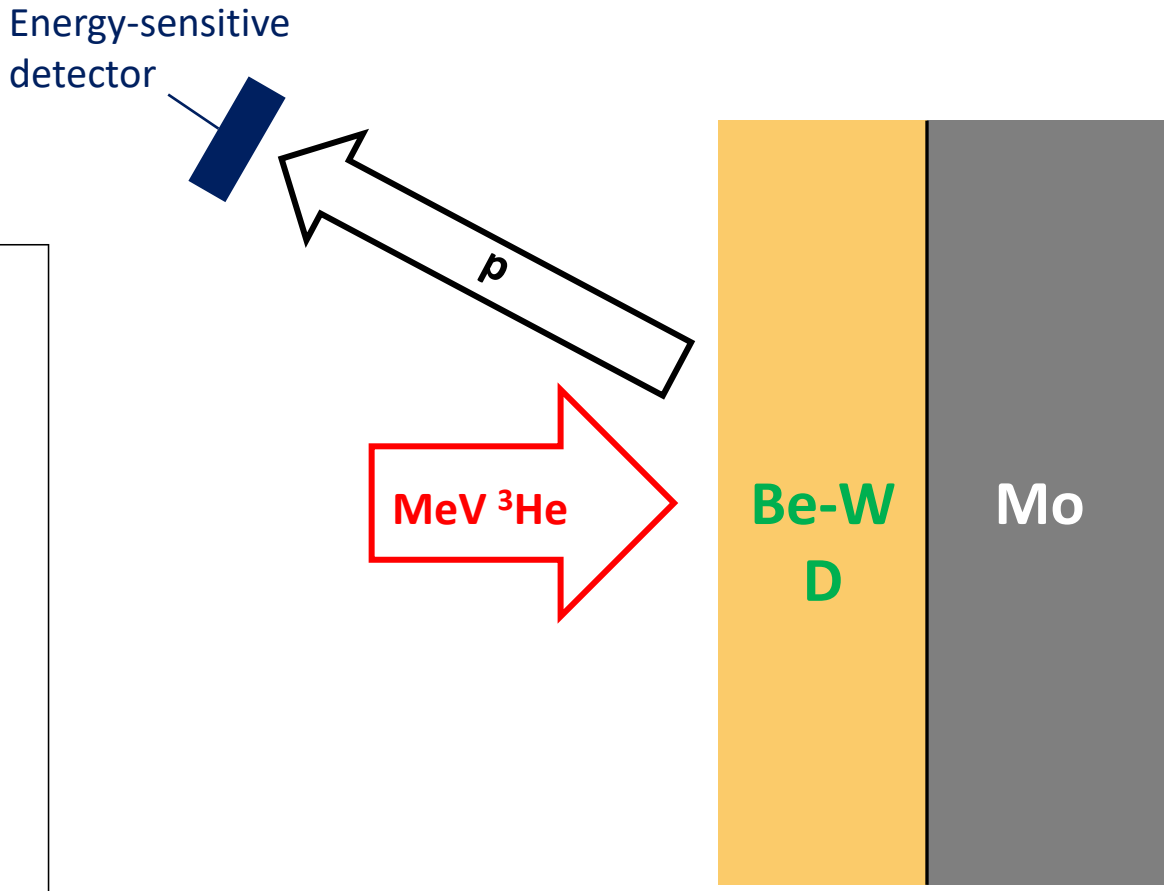

- Fitting of measured energy spectra in SIMNRA 7

Layer analyses

- Thermal desorption spectroscopy (TDS)
  → D trapping states

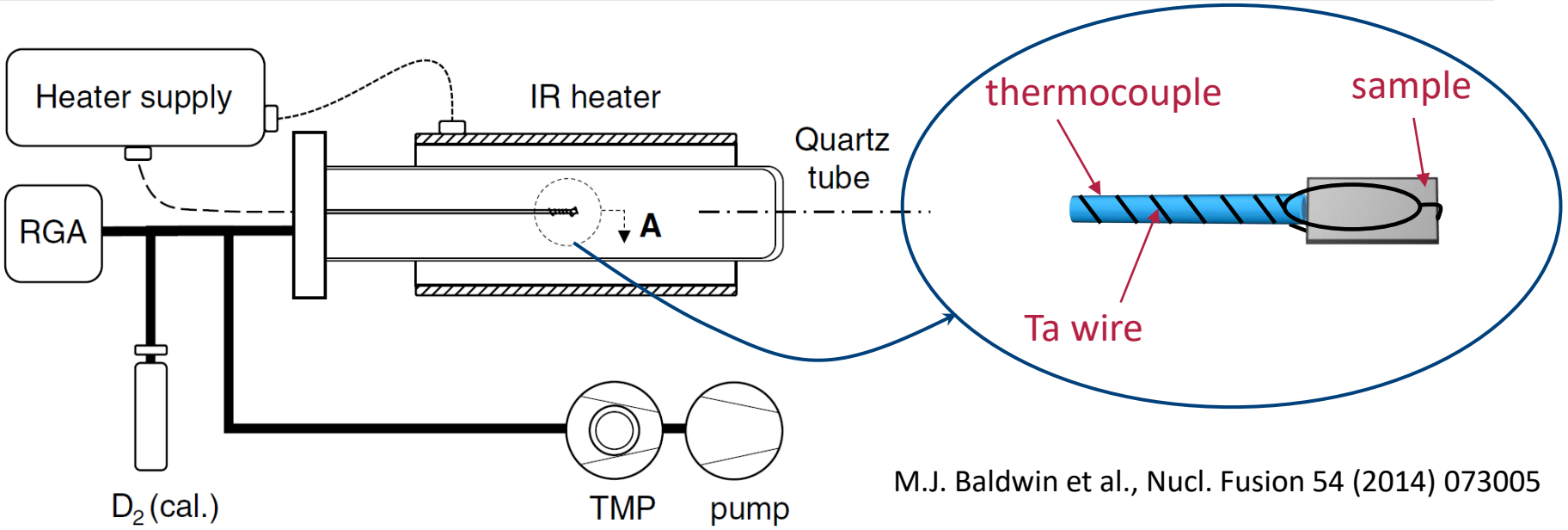

M.J. Baldwin et al., Nucl. Fusion 54 (2014) 073005

- SEM imaging of cross-sections of layers on Si
  → thickness, structure

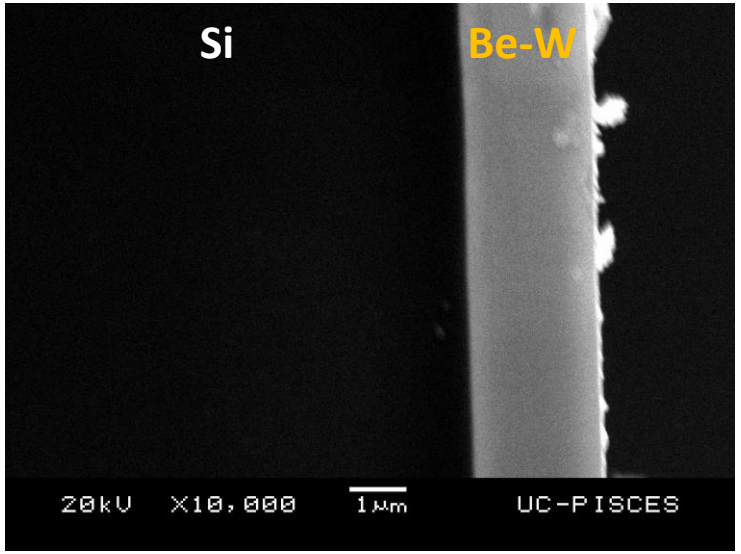

Microstructure of layers

Be-D layer:

- (002) orientation texture

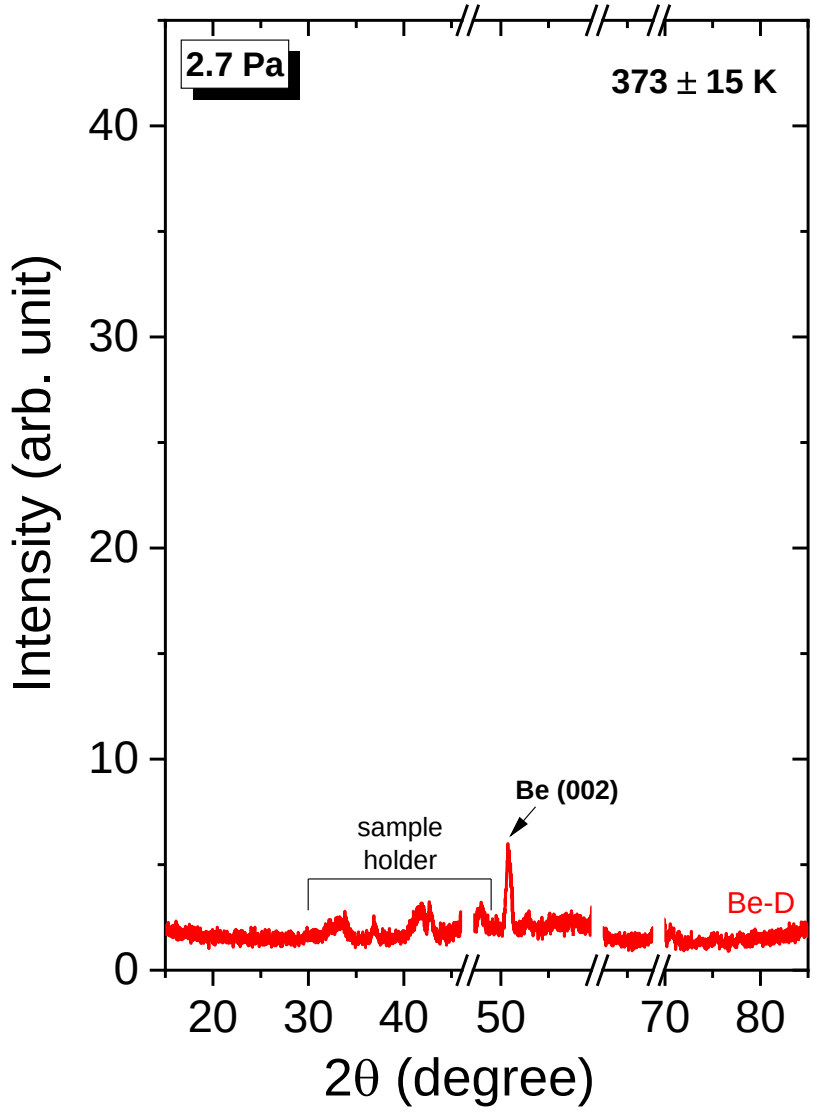

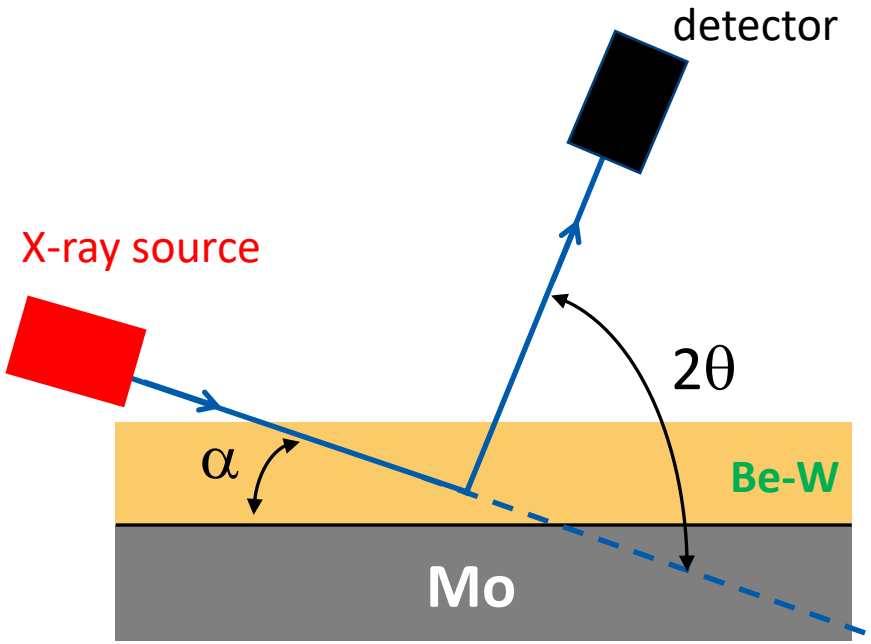

$\alpha = 5°$ (fixed)

Grazing incidence to increase X-ray path length in layers
→ decrease substrate contribution

Microstructure of layers

Be-D layer:

- (002) orientation texture
- columnar microstructure

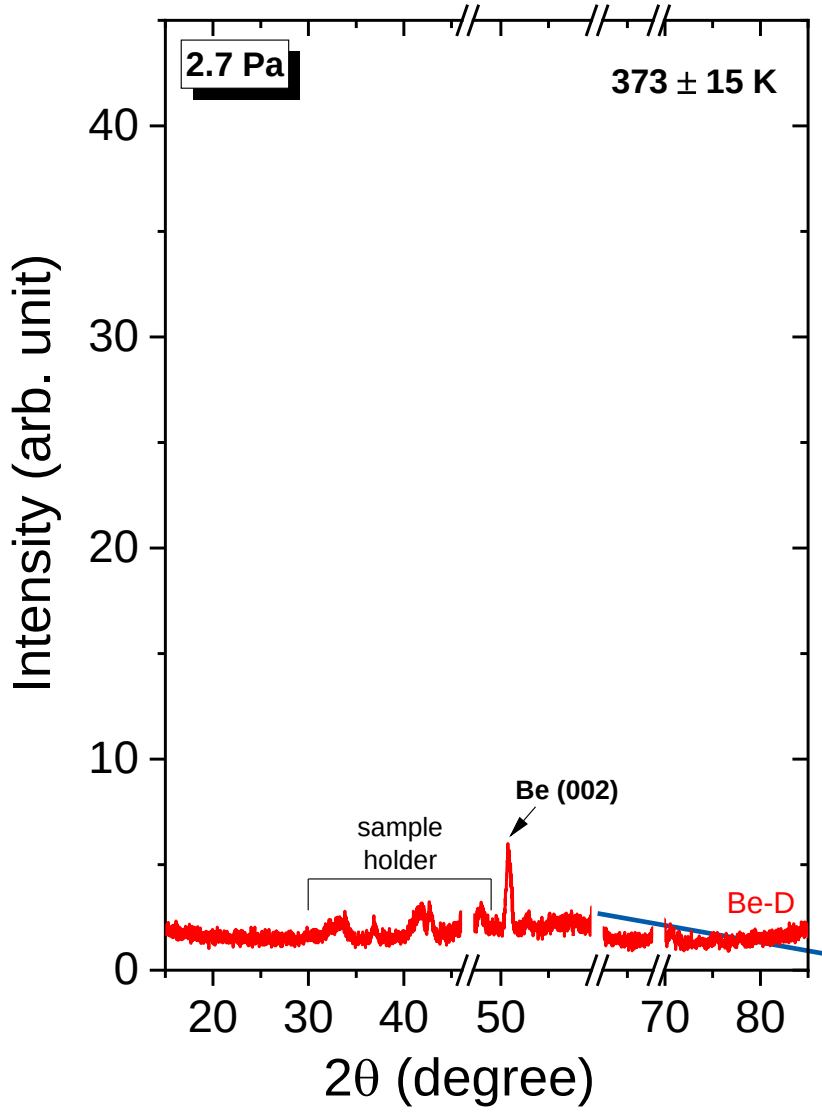

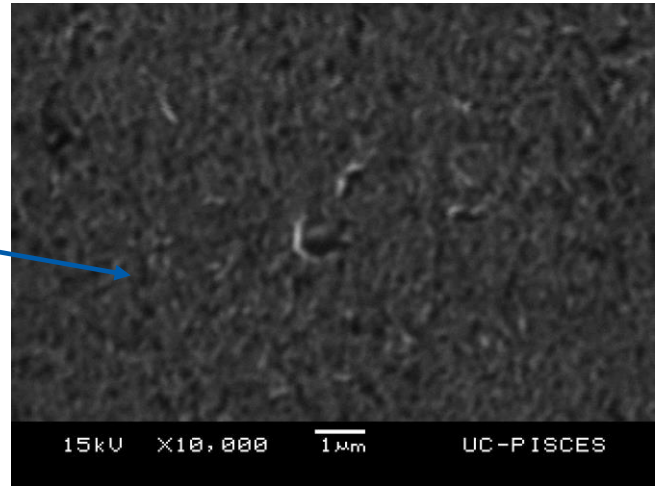

Microstructure of layers

Be-D layer:

- (002) orientation texture
- columnar microstructure

Be-W-D layers:

- amorphous

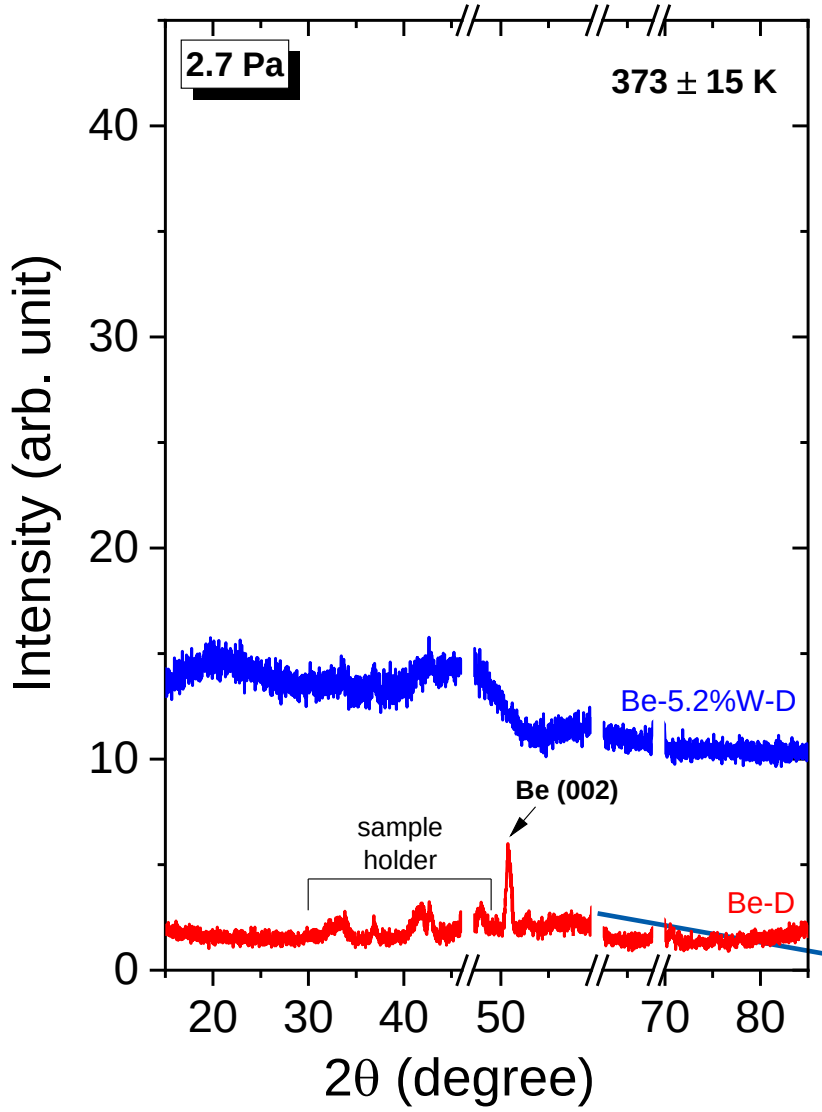

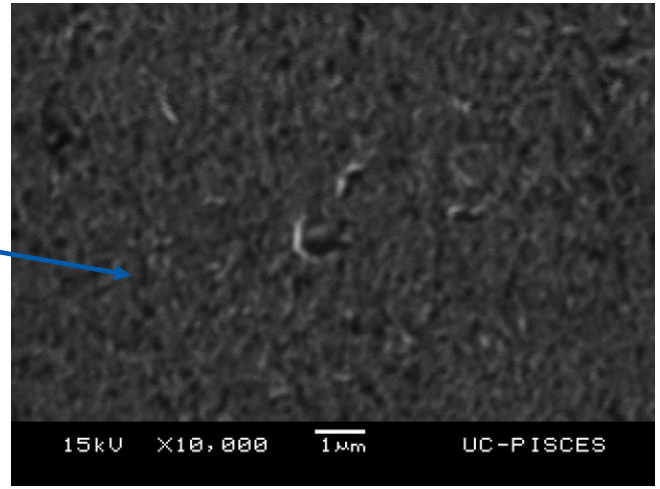

Microstructure of layers

Be-D layer:

- (002) orientation texture
- columnar microstructure

Be-W-D layers:

- amorphous
- no visible microstructure

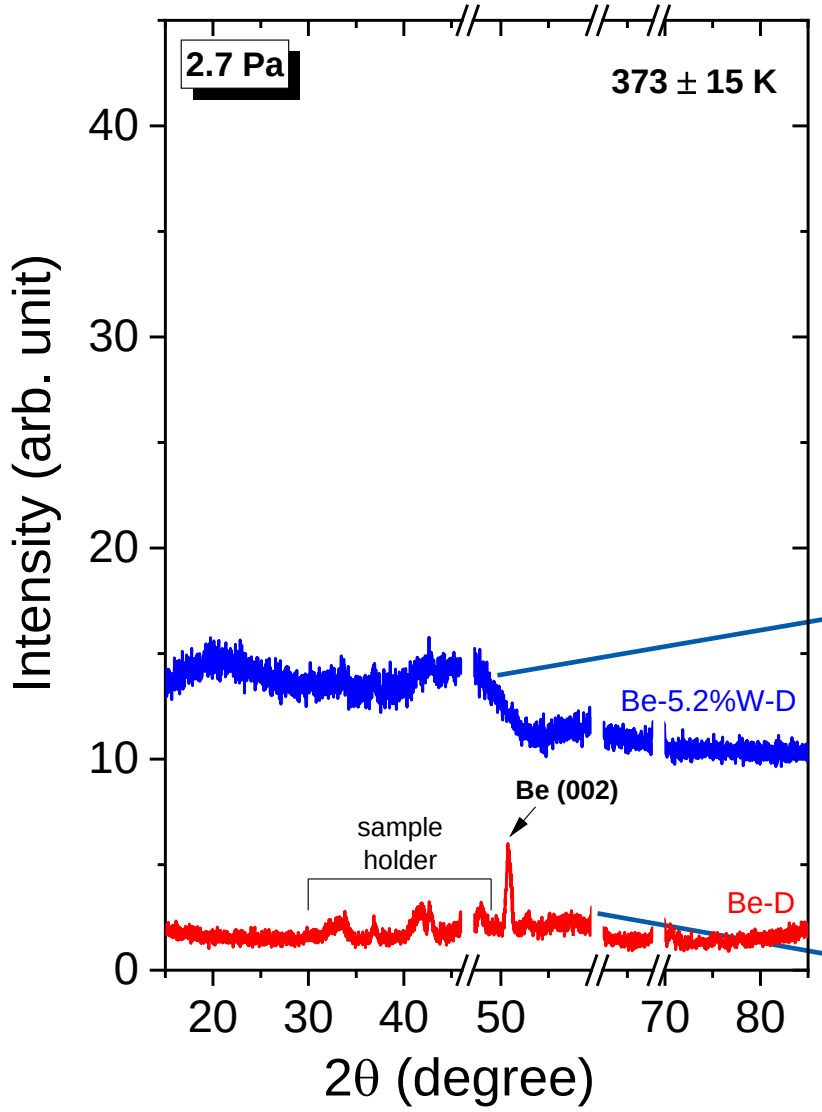

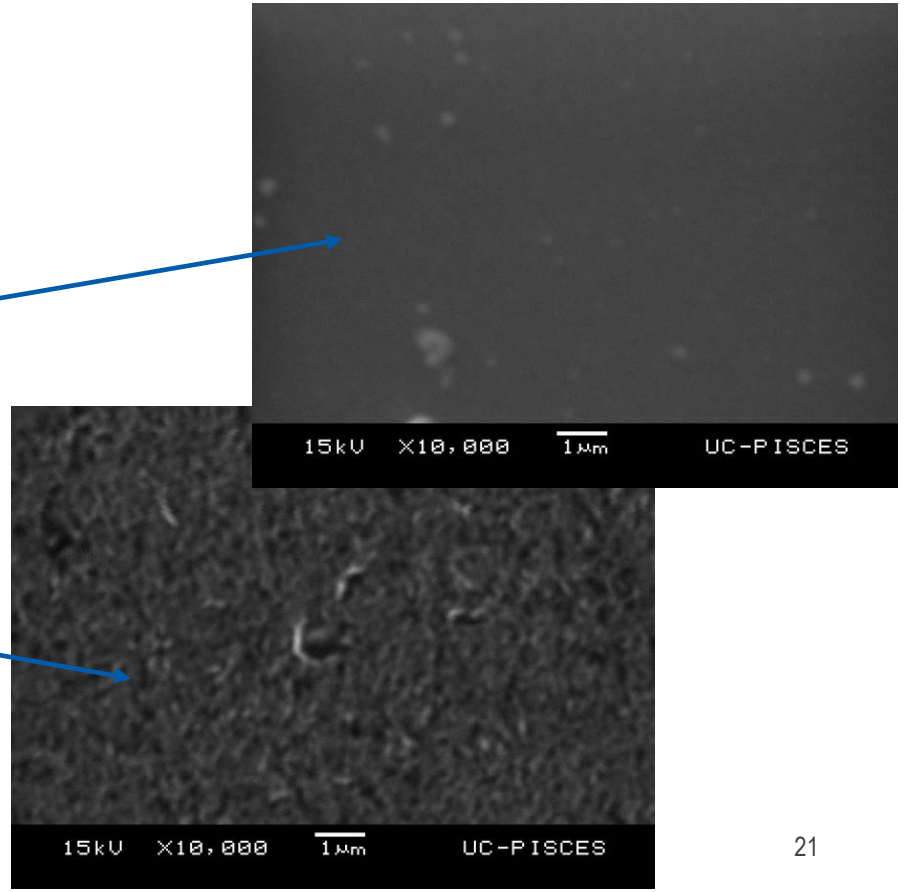

Microstructure of layers

Be-D layer:

- (002) orientation texture
- columnar microstructure

Be-W-D layers:

- amorphous
- no visible microstructure

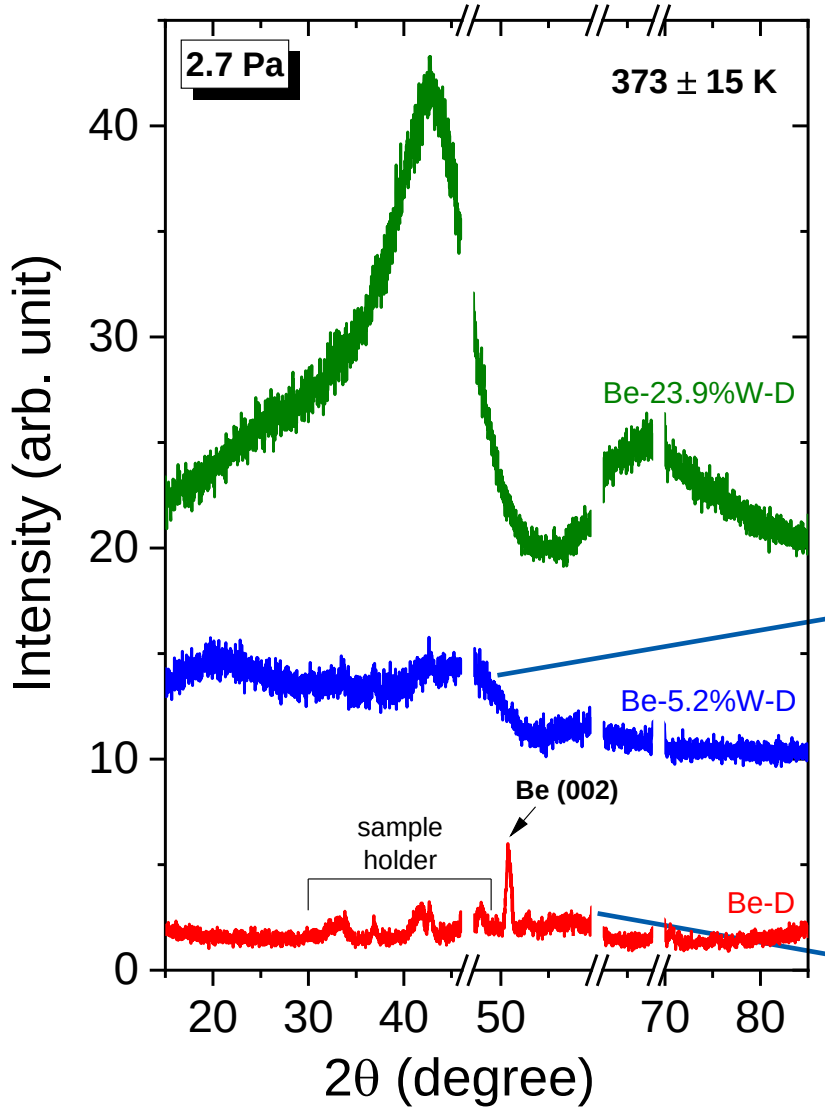

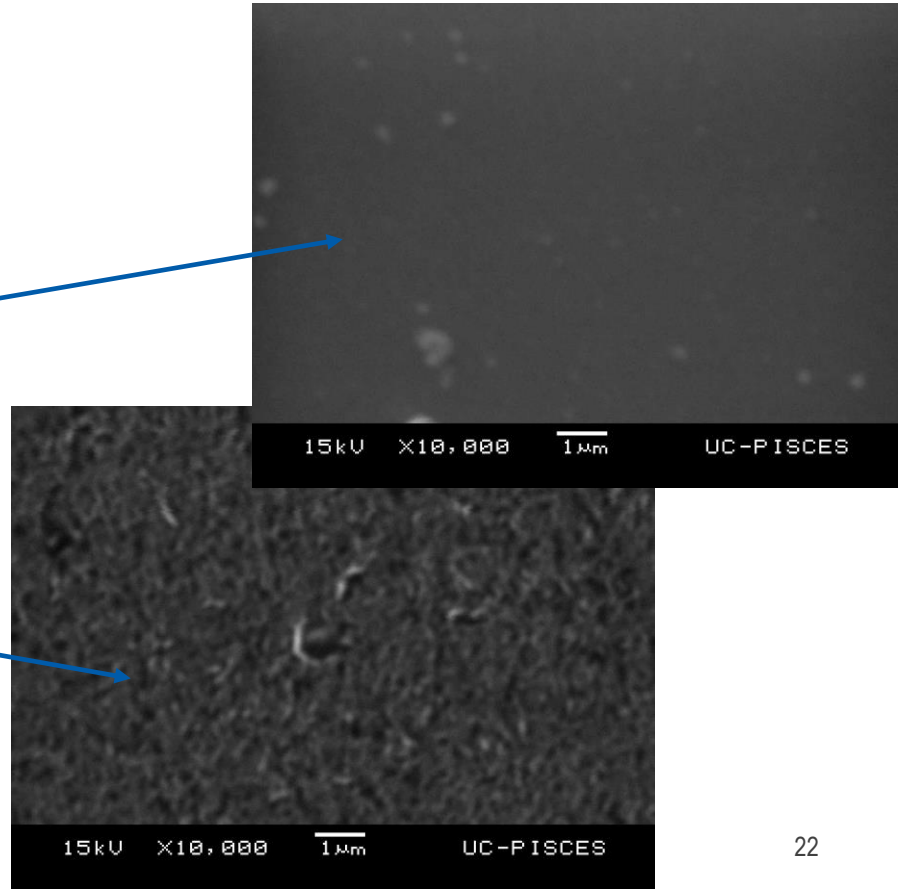

Microstructure of layers

Be-D layer:

- (002) orientation texture
- columnar microstructure

Be-W-D layers:

- amorphous
- no visible microstructure

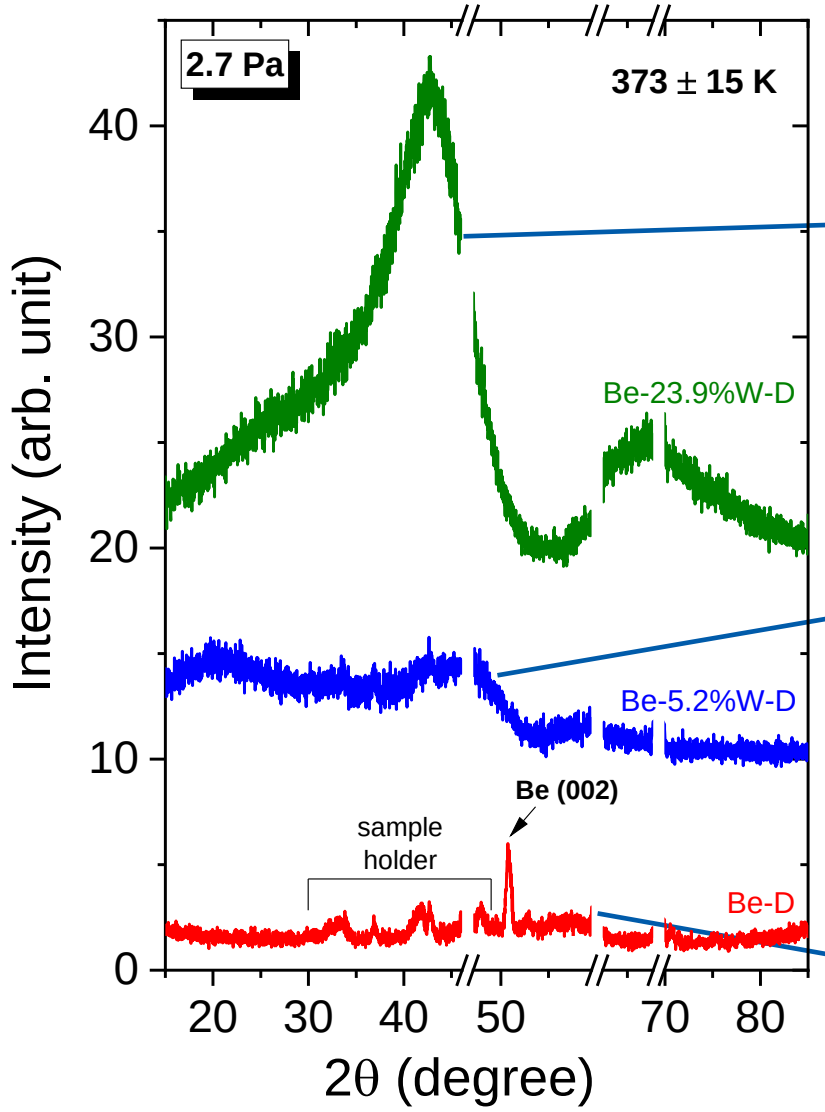

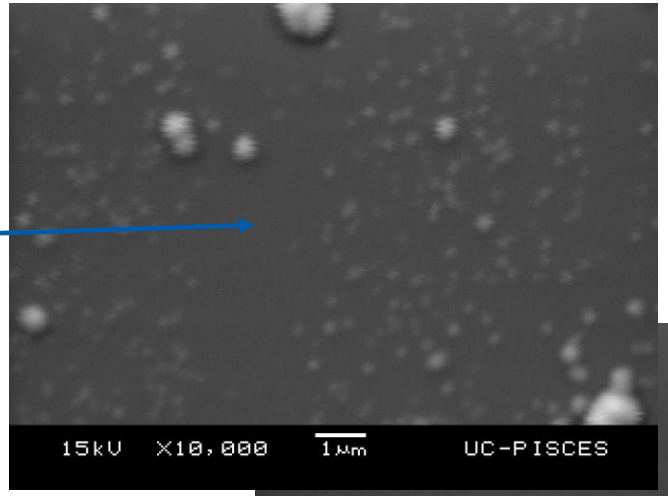

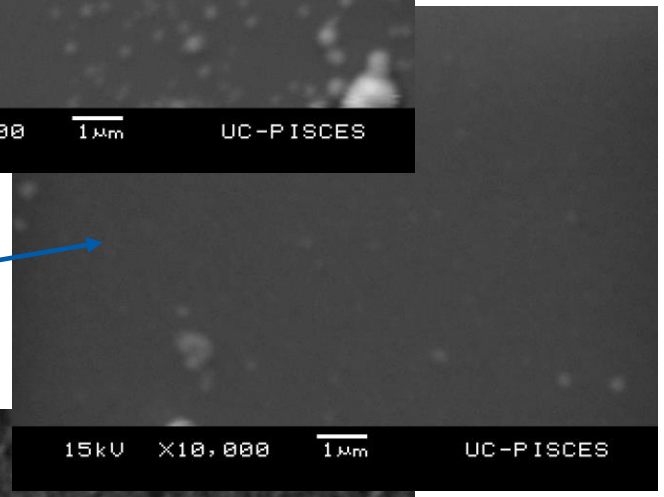

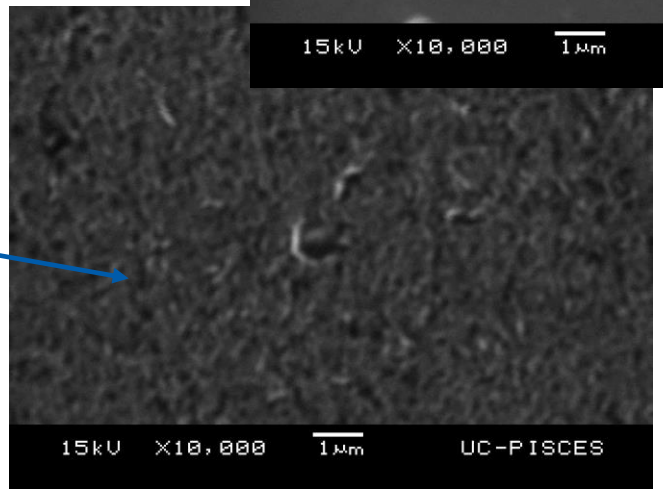

Microstructure of layers

Be-D layer:

- (002) orientation texture
- columnar microstructure

Be-W-D layers:

- amorphous
- no visible microstructure

W-D layer: columnar microstructure

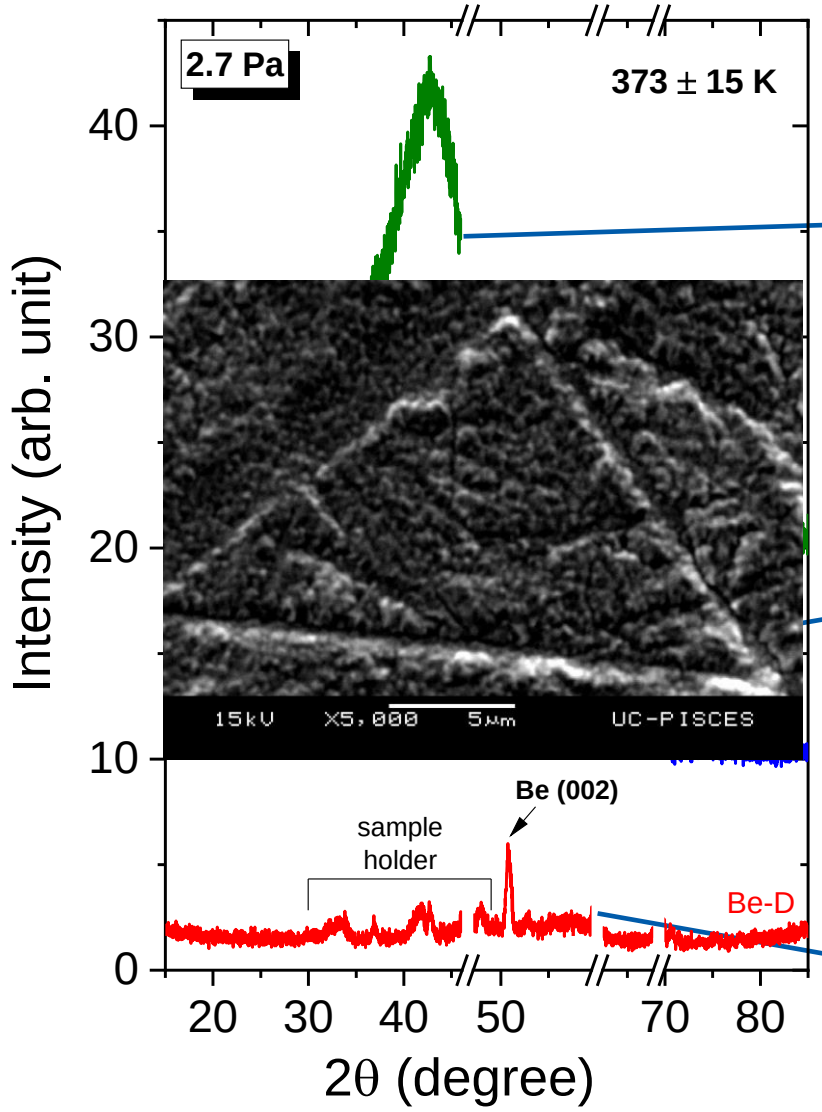

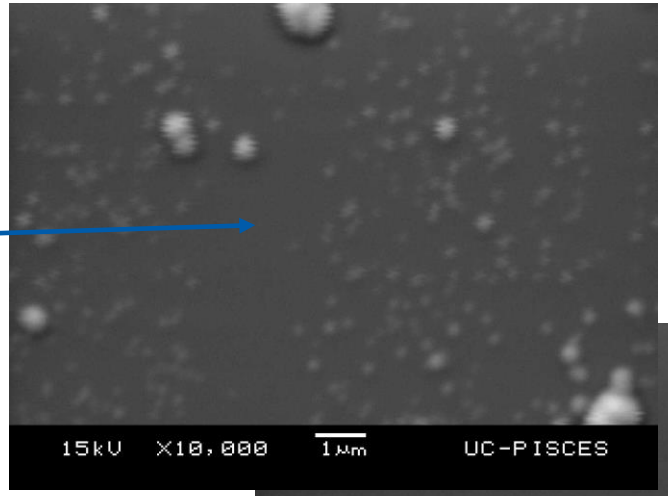

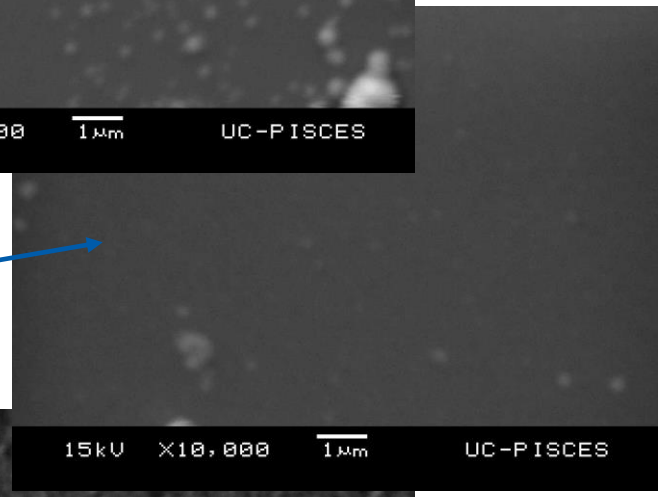

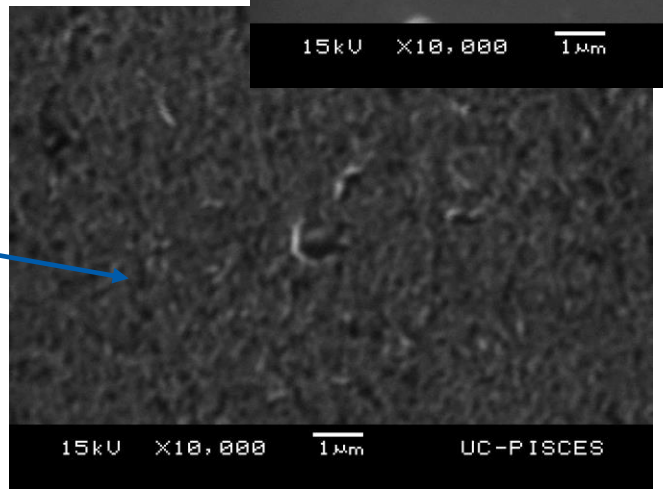

D concentration vs W concentration

- Non-monotonic dependence: maximum at 4–7% W
- Increase of D concentration in Be-D and Be-W-D layers (4–7% W) with increasing gas pressure
- D concentration in Be-D and W-D layers agrees with literature data

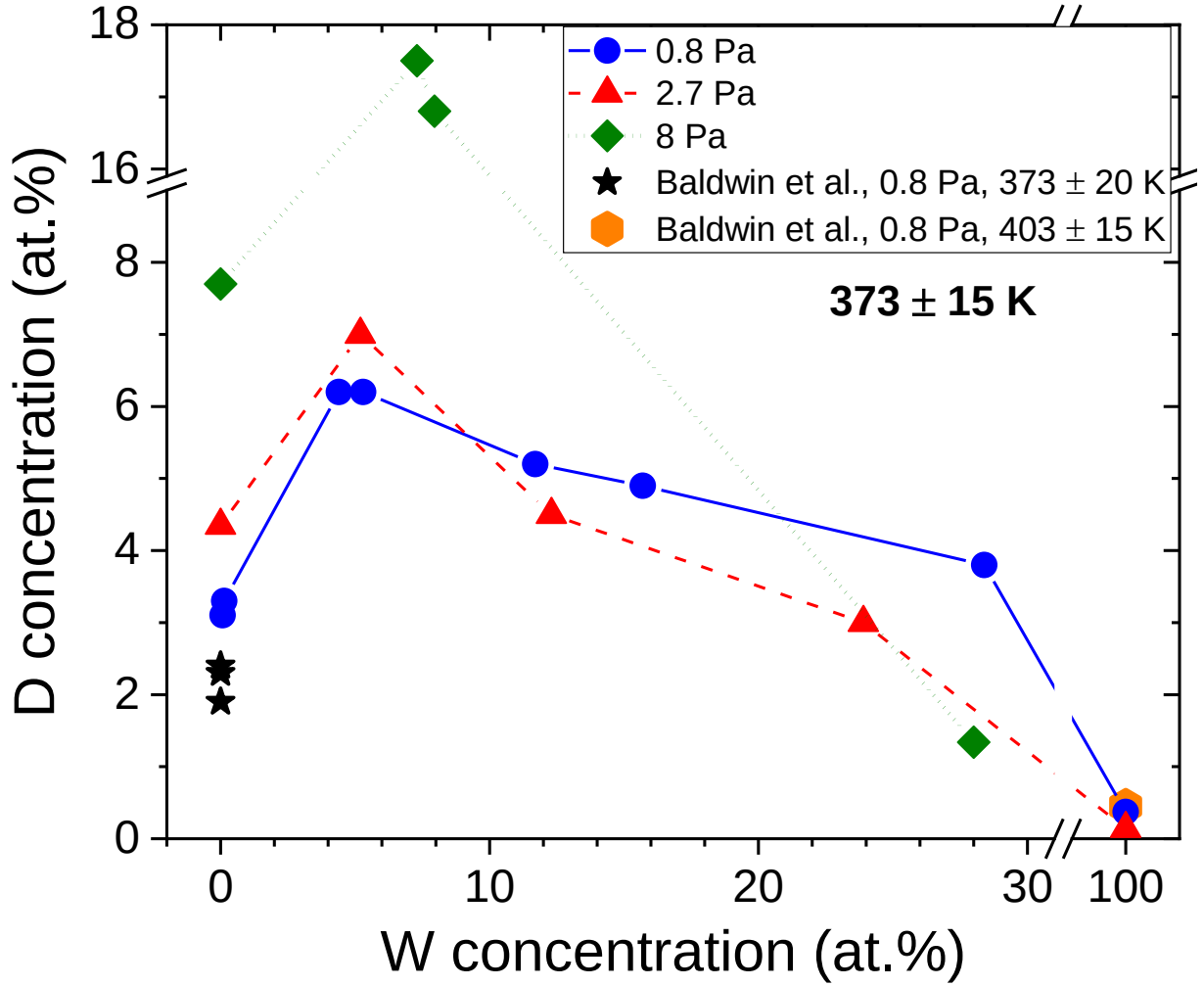

D thermal release

- **0% W (Be-D)**: appearance of sharp low-temperature peaks with increasing pressure

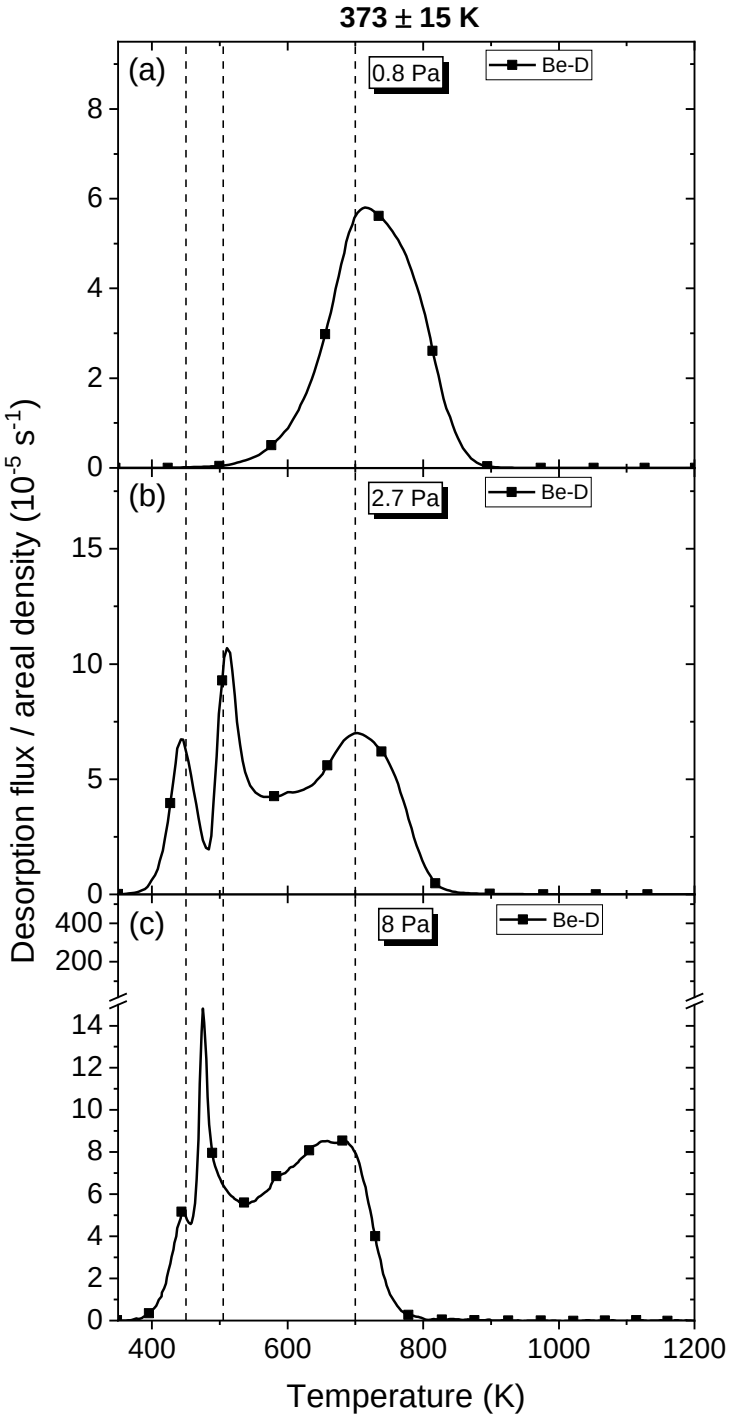

D thermal release

- **0% W (Be-D)**: appearance of sharp low-temperature peaks with increasing pressure
- **4.4–11.7% W**: mainly increase of amplitudes of low-temperature peaks

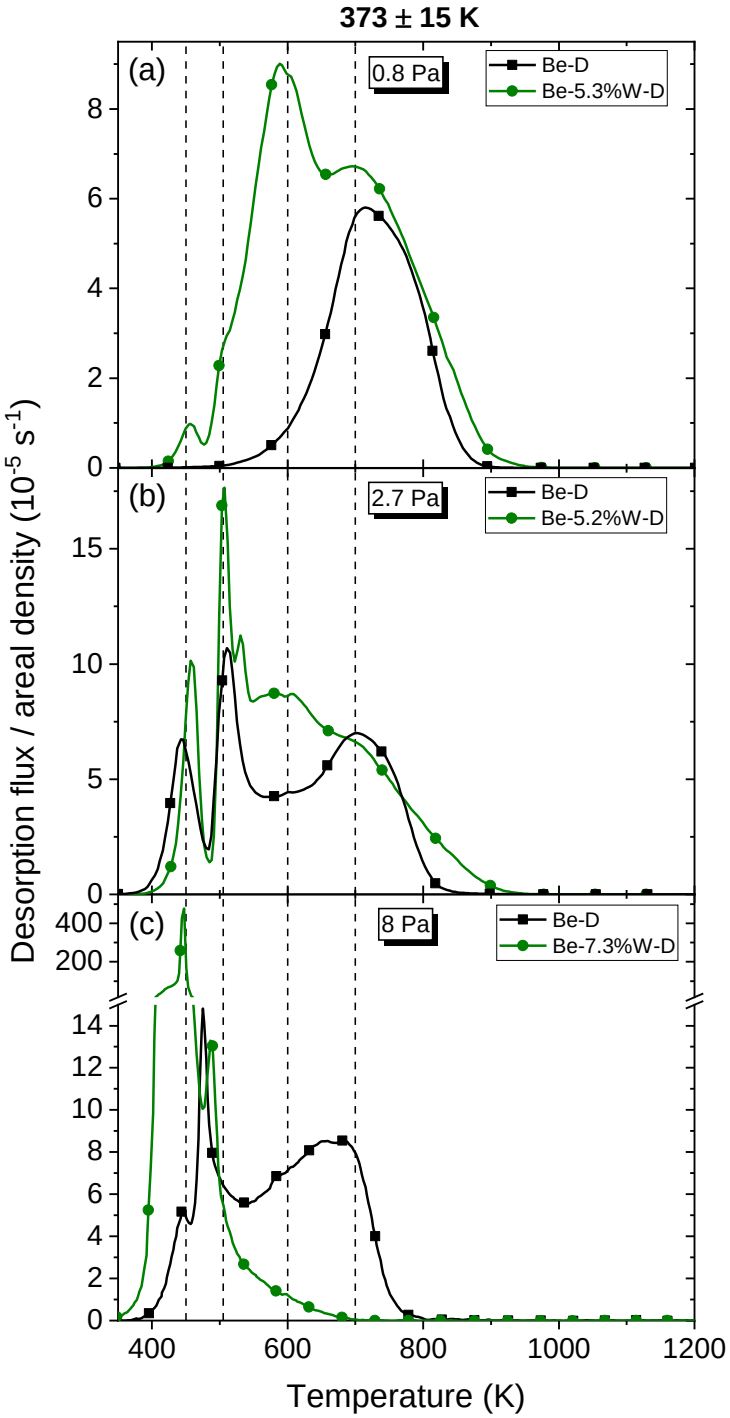

D thermal release

- **0% W (Be-D)**: appearance of sharp low-temperature peaks with increasing pressure
- **4.4–11.7% W**: mainly increase of amplitudes of low-temperature peaks
- **12.3–28.4% W**: disappearance of low-temperature peaks.

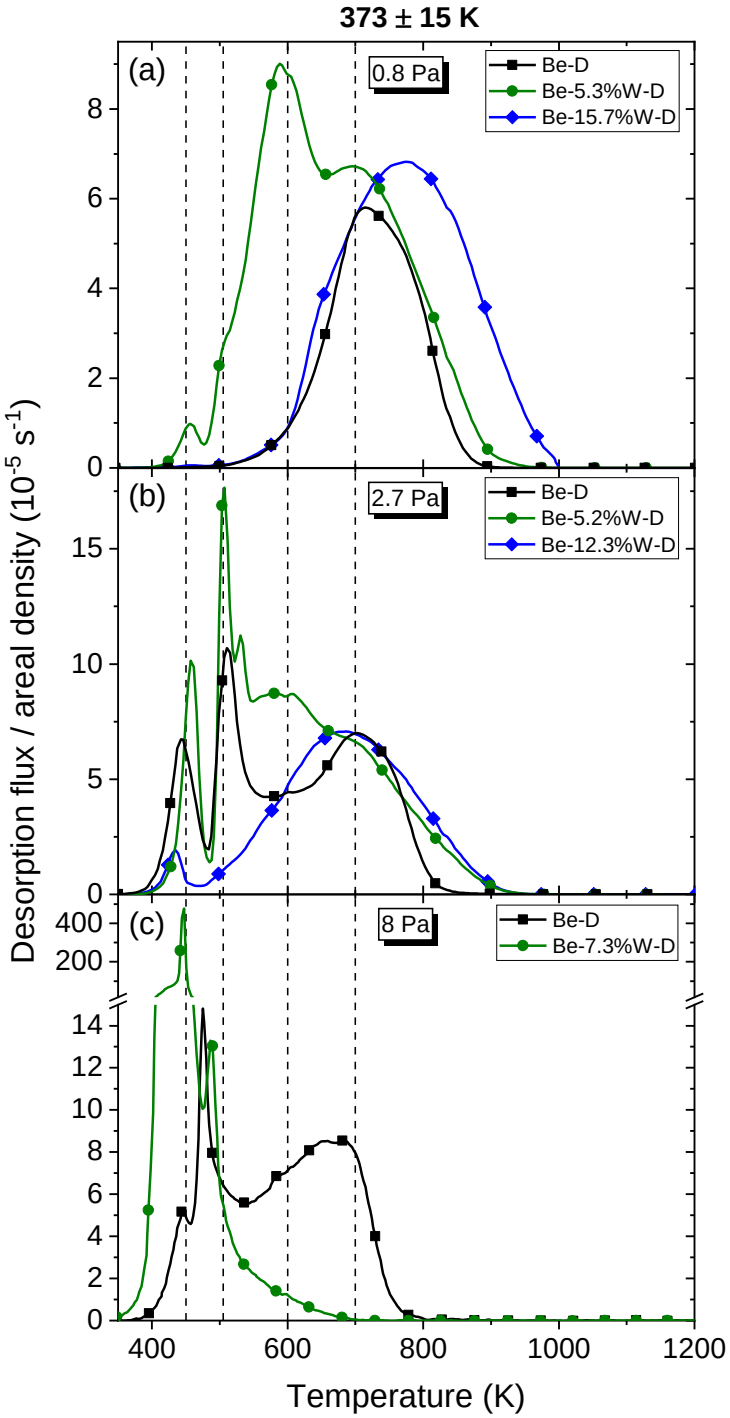

D thermal release

- **0% W (Be-D)**: appearance of sharp low-temperature peaks with increasing pressure
- **4.4–11.7% W**: mainly increase of amplitudes of low-temperature peaks
- **12.3–28.4% W**: disappearance of low-temperature peaks. Shift of desorption maximum towards higher temperatures at 0.8 Pa and 2.7 Pa

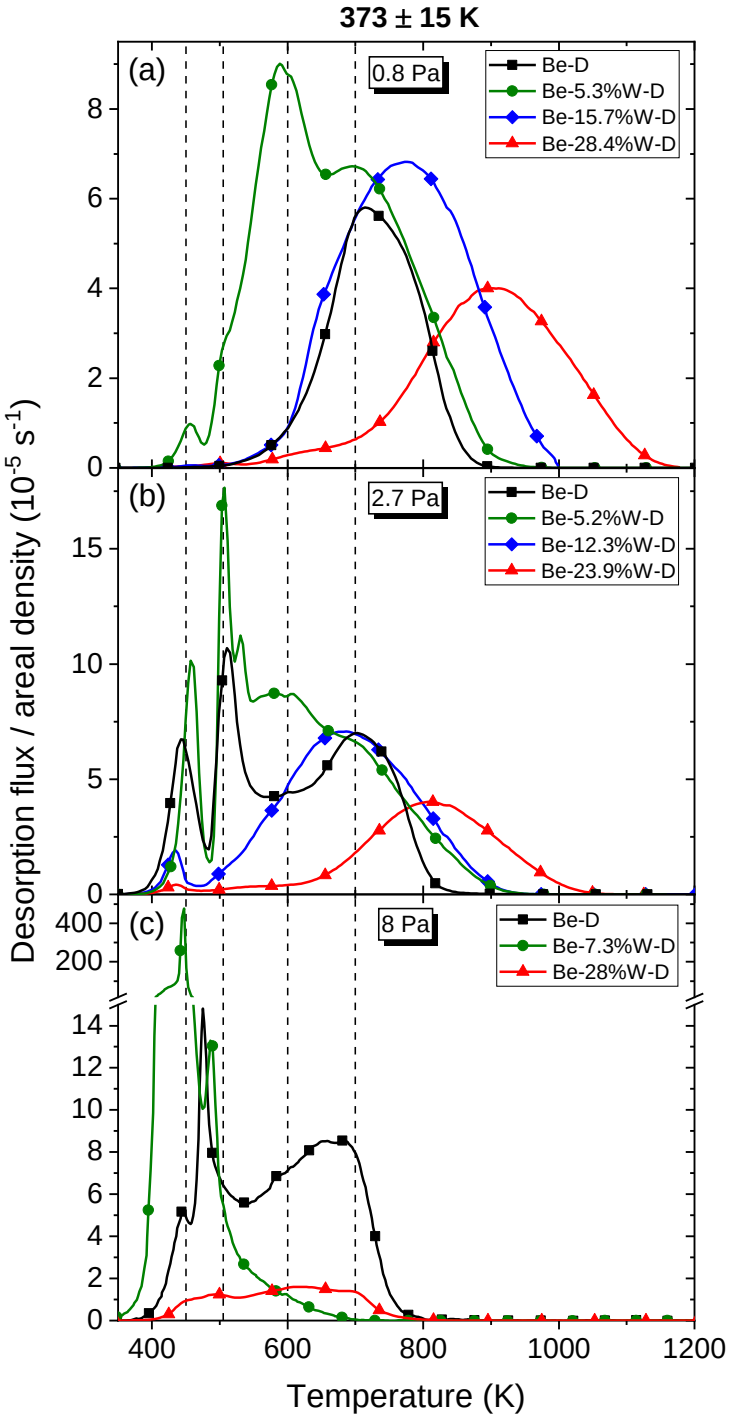

Simulated strike point sweeping D removal from Be-D co-deposited layers.

Experiment

- 3 batches of 4 Be-D co-deposits layer created by magnetron sputtering technique at 443 K
- ≈ 3 μm thick Be-D layers
- 1 sample from each batch was a control → went directly to TDS
- other samples were exposed to D or H plasma in PISCES-B, then TDS

	plasma	T_{exp} [K]	$t_{\uparrow}$ [s]	t_{exp} [s]
batch 1	D	773	245	180
				600
				1200
batch 2	H	773	245	200
				600
	no plasma			600
batch 3	D	673	385	180
		773		
		873		
pure Be	D	773	290	1200

T_{exp} is exposure temperature; $t_{\uparrow}$ is time needed to reach the exposure temperature; t_{exp} is exposure time at the exposure temperature; "no plasma": sample was only thermally treated, not exposed to plasma

Results

- exponential decrease of remaining D:
  - D plasma: 45%, 21% and 15% after 180 s, 600 s and 1200 s
  - H plasma: 30% and 12% after 200 s and 600 s
- ≈ 10% higher efficiency in the case of H plasma exposure compared to D plasma exposure
- rapid decrease of the remaining D with temperature:
  - 73%, 50% and 16% after exposure at 673 K, 773 K and 873 K
- this study illustrates the feasibility of plasma-induced removal as potential means of T control, but some open questions remain:
  - How high can the strike-points be raised?
  - How much power can be coupled in such configuration?
  - Where will the T-rich co-deposits actually form? Will they be accessible?

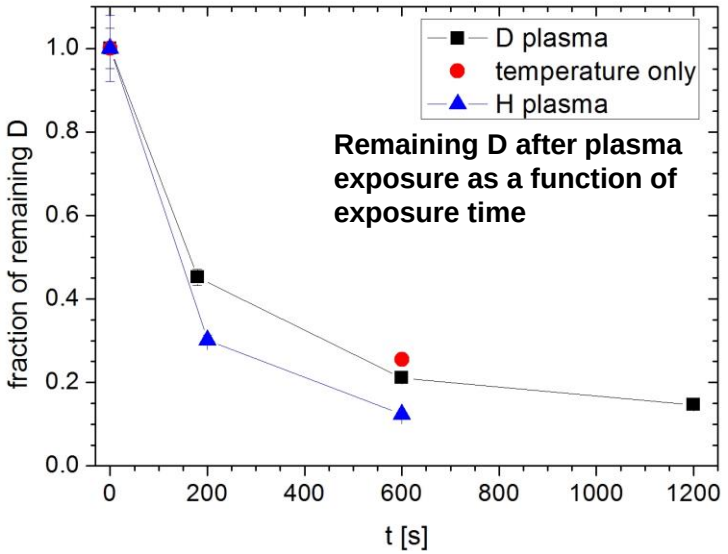

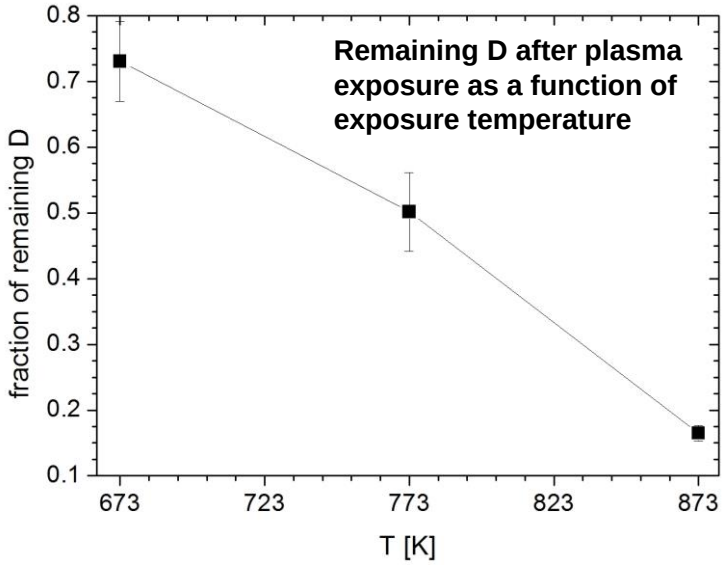

Studies of D retention in damaged Be.

Experiment

- Be samples irradiated by high-energy O ions (6 different energies) up to 0.01 dpa, 0.1 dpa, and 1 dpa (at IPP)
- D plasma exposure at 370 K and 573 K, fluence 10^{26} D/m^2
- NRA for D depth profiling with 2000 keV, 800 keV, and 500 keV ^{3}He ion beam (at IPP)
- TDS on samples, exposed at 370 K and 1 sample exposed at 573 K, damaged up to 0.01 dpa; heating rate 0.3 K/s
- TEM on samples exposed at 573 K and damaged up to 0 dpa, 0.1 dpa, and 1 dpa, then TDS, but only D_2 recorded; heating rate 1 K/s (at Shimane University)

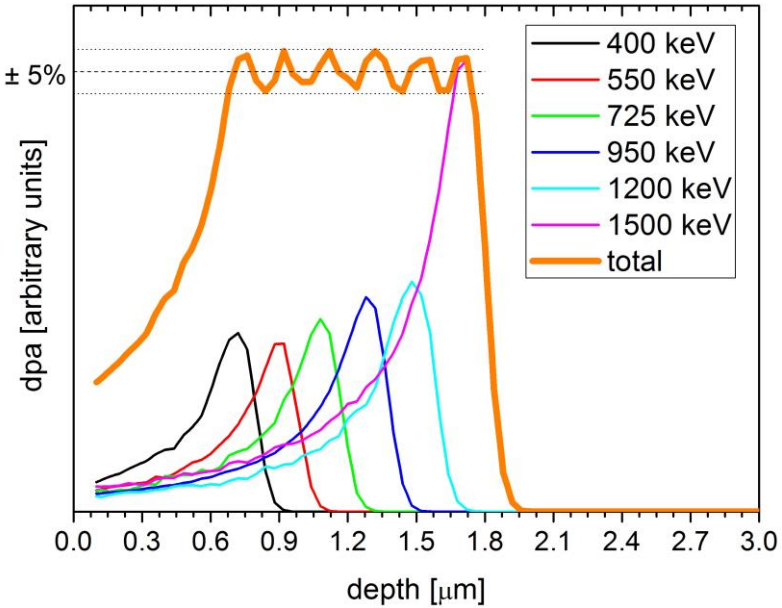

The damage profile after O ion irradiation with 6 different energies as calculated by SRIM software.

Results

- TDS of samples exposed at 370 K:
  - 4 peaks, the first peak increasing with dpa, other three decreasing
  - similar behavior in samples exposed at 573 K with the onset temperature shifted accordingly
- Total D amounts:
  - NRA and TDS agree relatively well within the uncertainties
  - D retention decreases with dpa, but saturates; not much change between 0.1 dpa and 1 dpa
- The results indicate that plasma exposure creates considerable amount of defects, governing the retention
- The observed decrease of D retention could be explained by ion-damage assisted growth of large networks of interconnected bubbles, opening toward the surface and reducing D retention

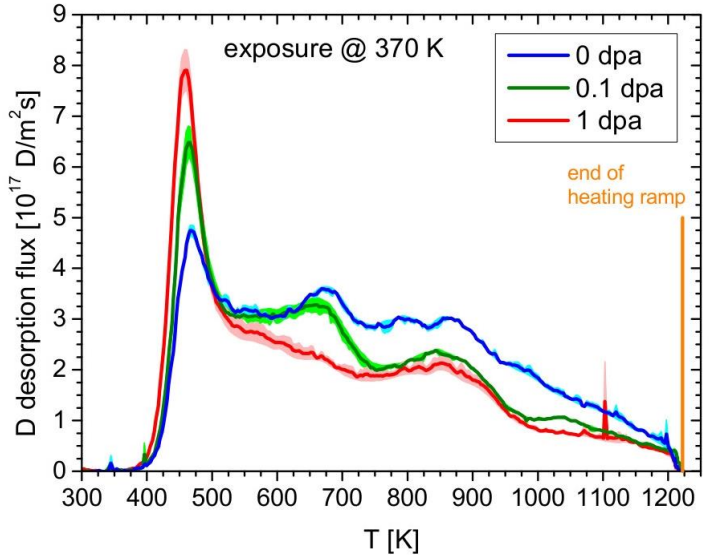

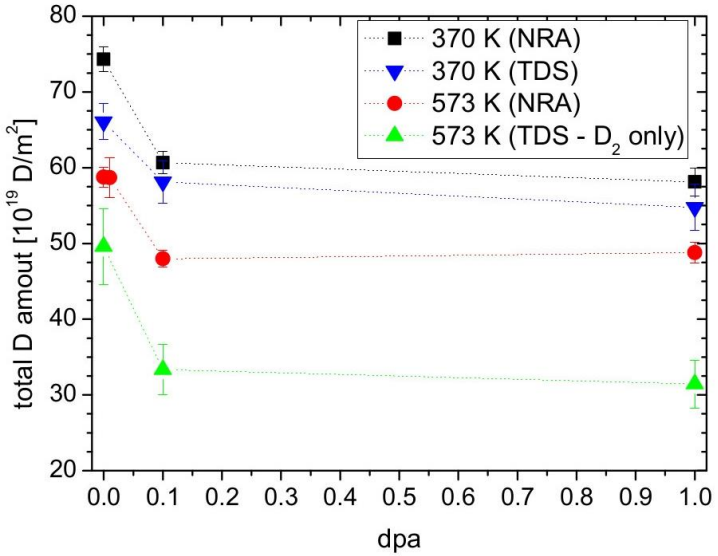

D retention in RAFM steels

Counter-intuitive fluence dependence of D retention in RAFM steels can be explained by the Cr content in the surface layer.

- Outgassing at 773 K for 1 h before plasma exposure causes a Cr-rich surface layer.
- **The Cr concentration on the surface decreases with an increase in the fluence due to sputtering** during plasma exposure.

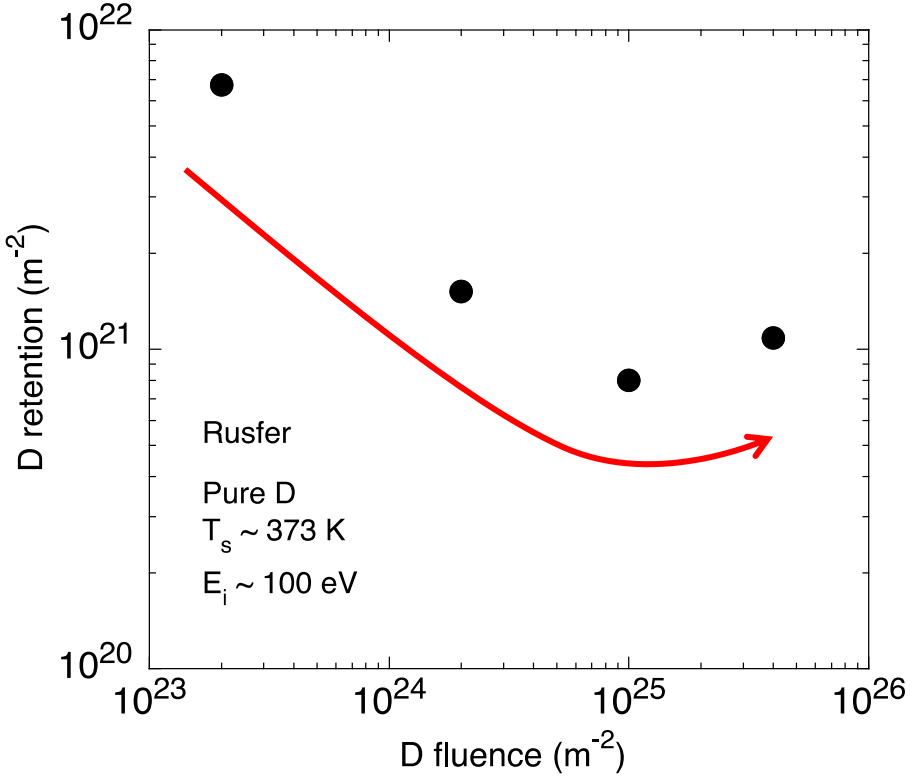

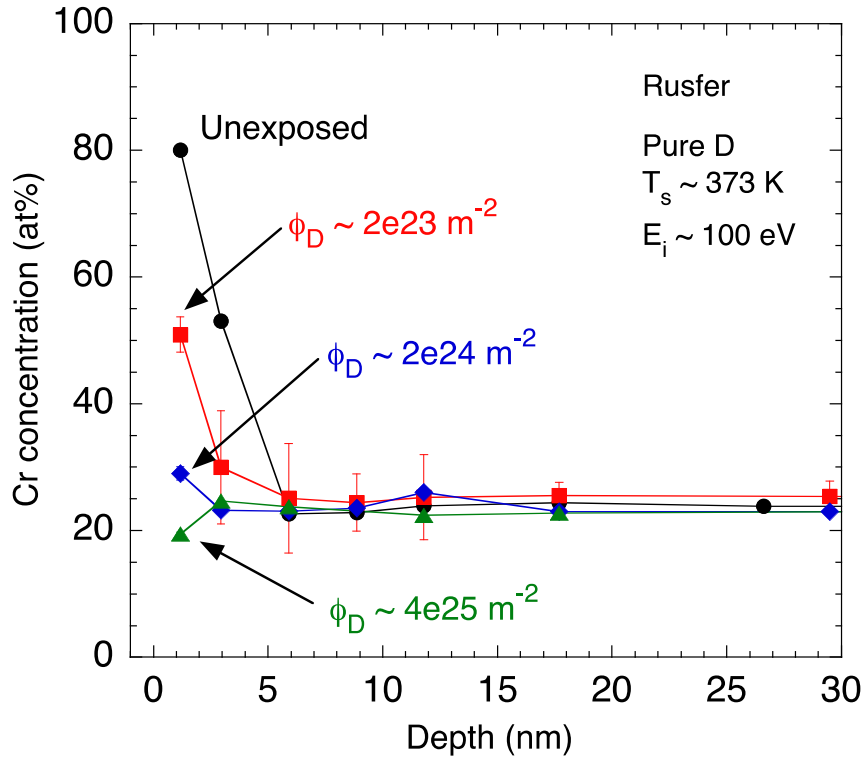

D. Nishijima et al., Phys. Scr. 2020

As with He, Ar seeding reduces the D retention in RAFM steels, while the D retention significantly increases with N_2 seeding.

PISCES

- **The low temperature peak is more sensitive to seeding of Ar and N_2 impurities**, as observed with He seeding.
- A **N-rich surface layer** (~10 nm thick) was formed during D+N plasma exposure, and is thought to be **responsible for the enhanced D retention**.

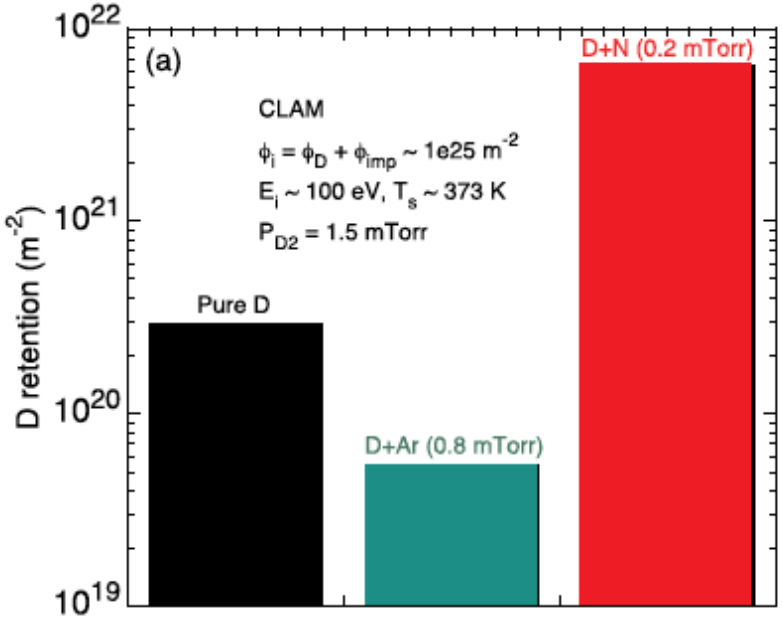

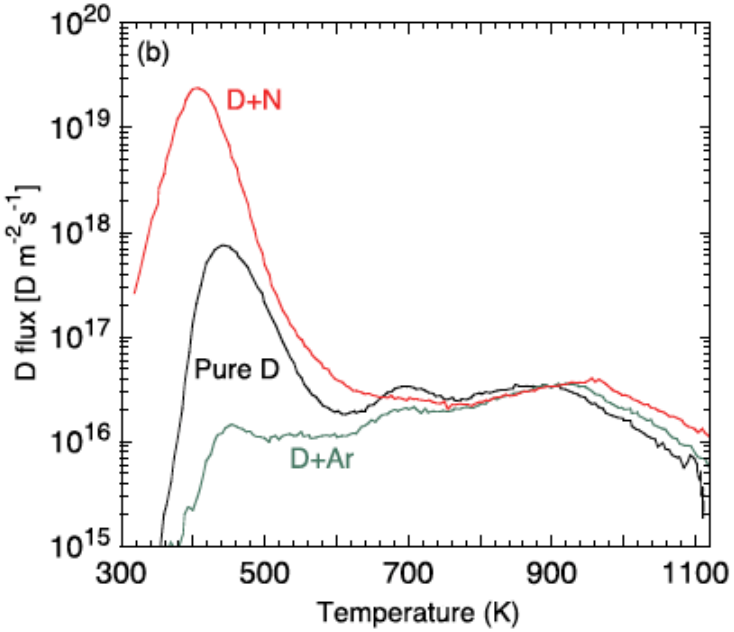

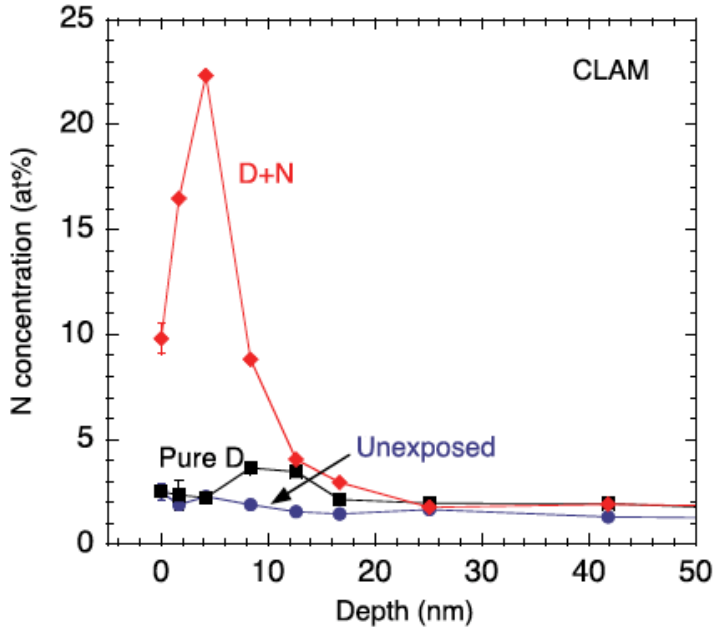

D. Nishijima et al., Nuclear Materials and Energy 2020

In-situ diagnostic development: Ongoing LIBS experiments

The upgraded in-situ LIBS system on PISCES-A enables to quickly, precisely, and widely move the laser spot on the sample surface.

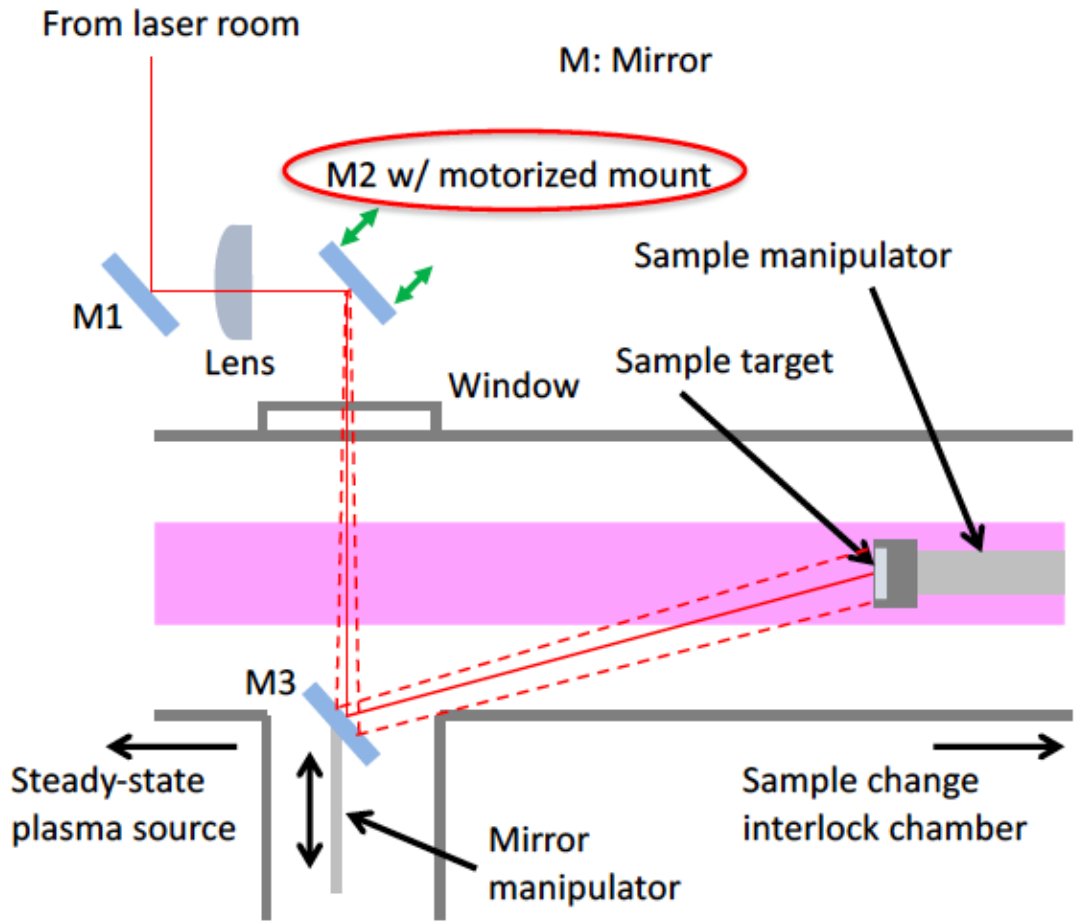

Sample surface after experiment

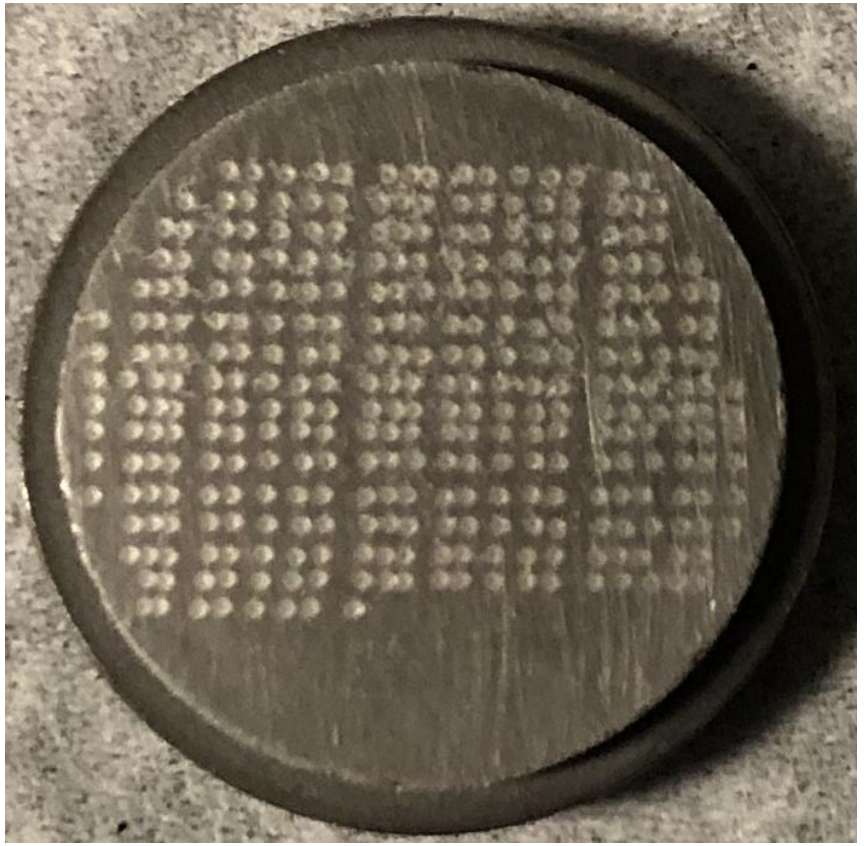

ϕ25 mm

It is found that dynamic retention of D in W gradually decreases with increasing T_s from 350 K to 475 K, and quickly drops at T_s > 475 K

- Laser energy: ~ 115 mJ
- Ablation depth: ~350 nm/shot
- Spot diameter: ~ 150 μm

- ICCD delay: t_{delay} ~ 10 ns (with respect to the time when a laser pulse hits the surface.)
- ICCD gate width: t_{width} = 2 μs

- 20 spectra (shots) were accumulated with one laser shot per spot.
- Multiple data sets were collected for each condition, and then the mean value and standard deviation (error bar) were calculated.

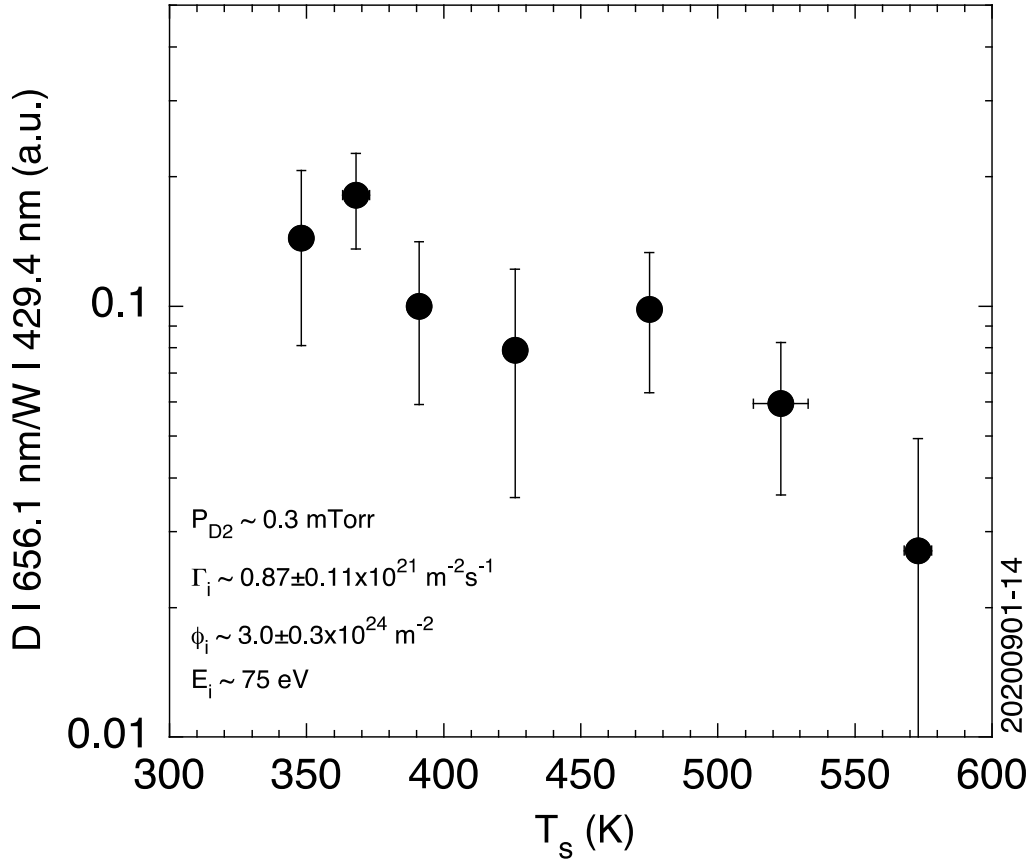

In-situ diagnostic development: HIS experiments

Hyperspectral imaging (HSI) is expected to become a powerful tool in plasma and fusion research, as in many other fields.

- **Each pixel of an HSI camera contains spectral data typically with more than a hundred bands, while it still records 2D images**.
- It is possible to **simultaneously obtain 2D images of multiple emission lines at different wavelengths** from a plasma.
- An HSI camera will easily **enable background/continuum emission light subtraction,** which is a **big advantage against conventional filter-cameras**.
- An HSI camera (**Specim IQ**) has been characterized for the **application in steady-state PMI experiments**.

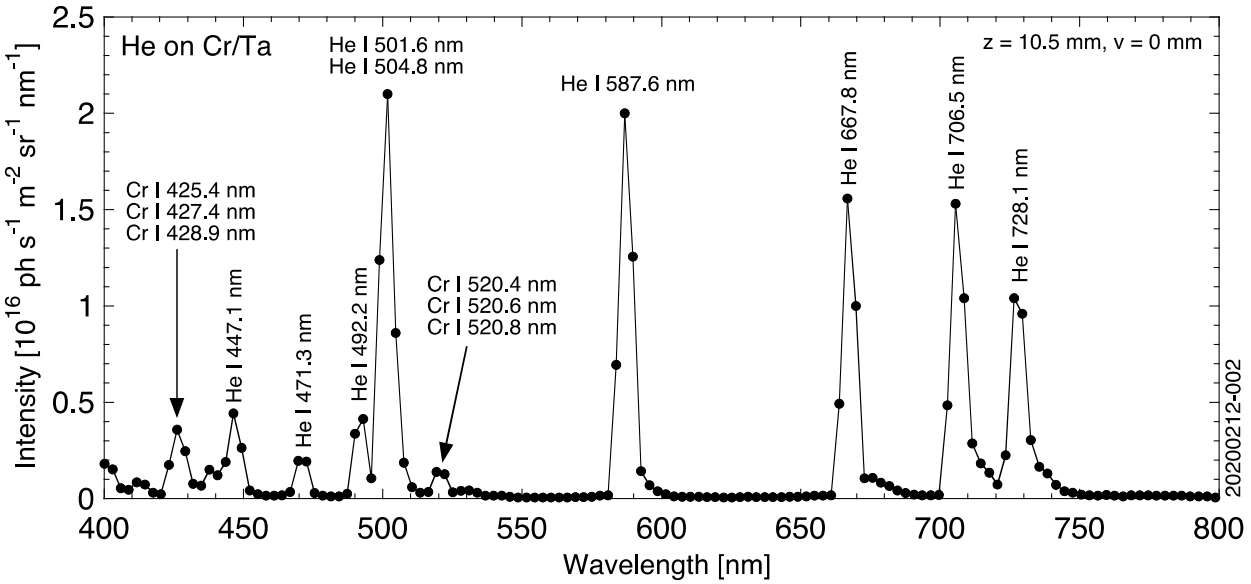

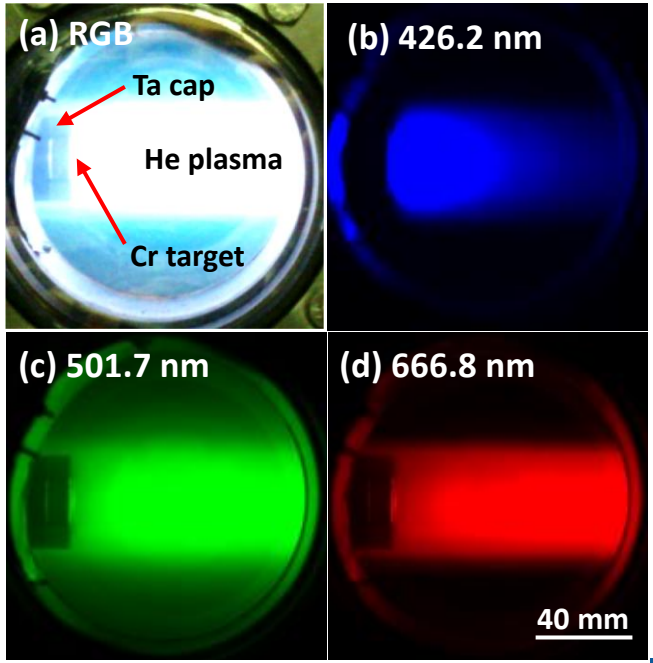

UC San Diego

D. Nishijima et al., Review of Scientific Instruments 2020

CER Center for Energy Research

Angular distribution of sputtered Cr atoms varies to the more forward ejection of Cr atoms, as cone structures grow on the surface.

PISCES

2D false color images of the total intensity of Cr I 426.9 nm after subtraction of background emission component

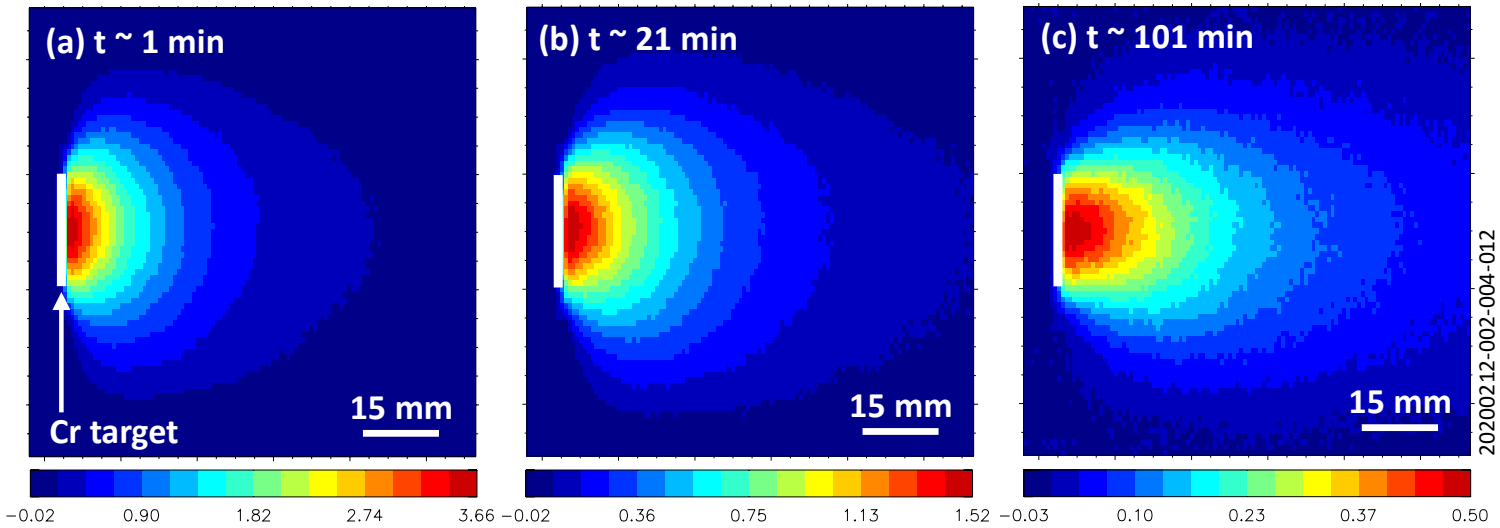

(d) Cr surface w/o plasma exposure

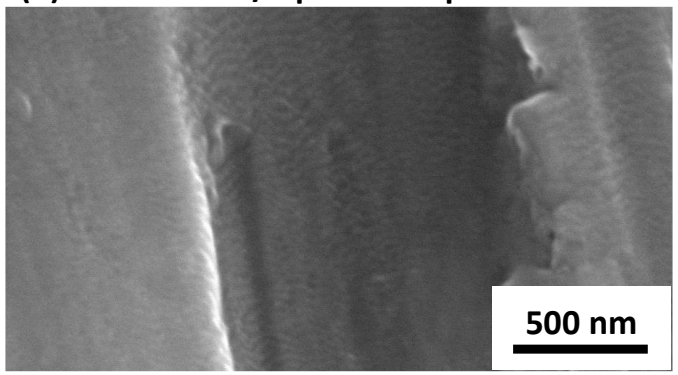

(e) Cr surface after plasma exposure

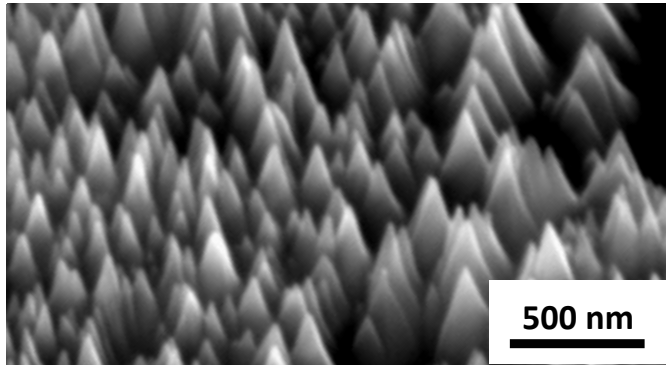

D. Nishijima et al., Review of Scientific Instruments 2020

- This observation is consistent with 1D (axial) profile measurements (at v = 0 mm) of Be I line emission intensity of sputtered Be atoms.

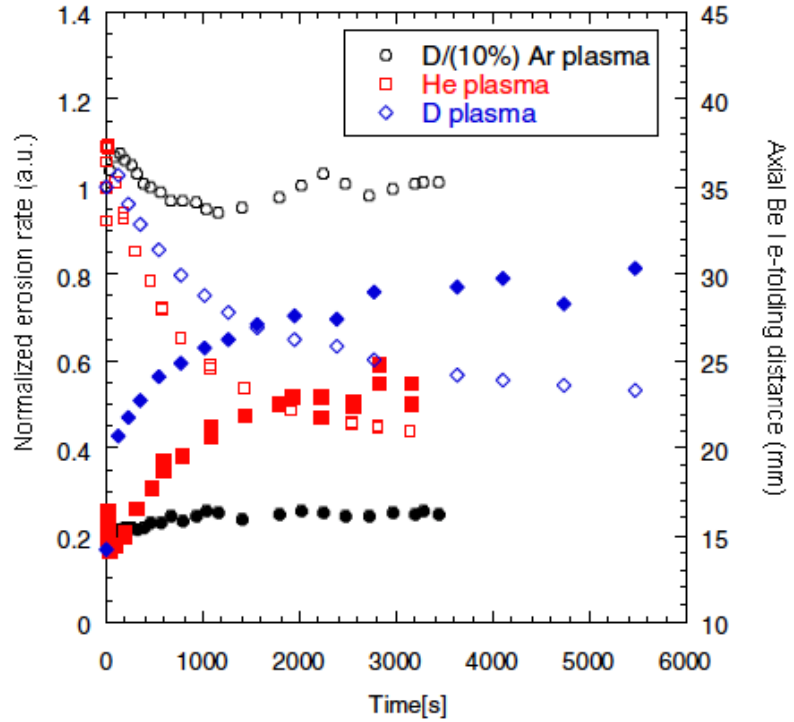

R.P. Doerner et al., Phys. Scr. 2014

UC San Diego

CER Center for Energy Research

ERO 2.0 validation of PISCES-B Be erosion

Experiments on Be erosion for the validation of ERO2.0 are ongoing in PISCES-B.

- D plasma exposure to Be: $\Gamma_i(0)$ ~ 2.0x10^{22} m^{-2}s^{-1}, $T_e(0)$ ~ 5 eV, $n_e(0)$ ~ 2x10^{18} m^{-3}, E_i ~ 85 eV
- Sample temperature scan
- Axial emission profiles of eroded Be atoms (Be I 457.3 nm) and BeD molecules (A-X band) are observed with a standard spectrometer.

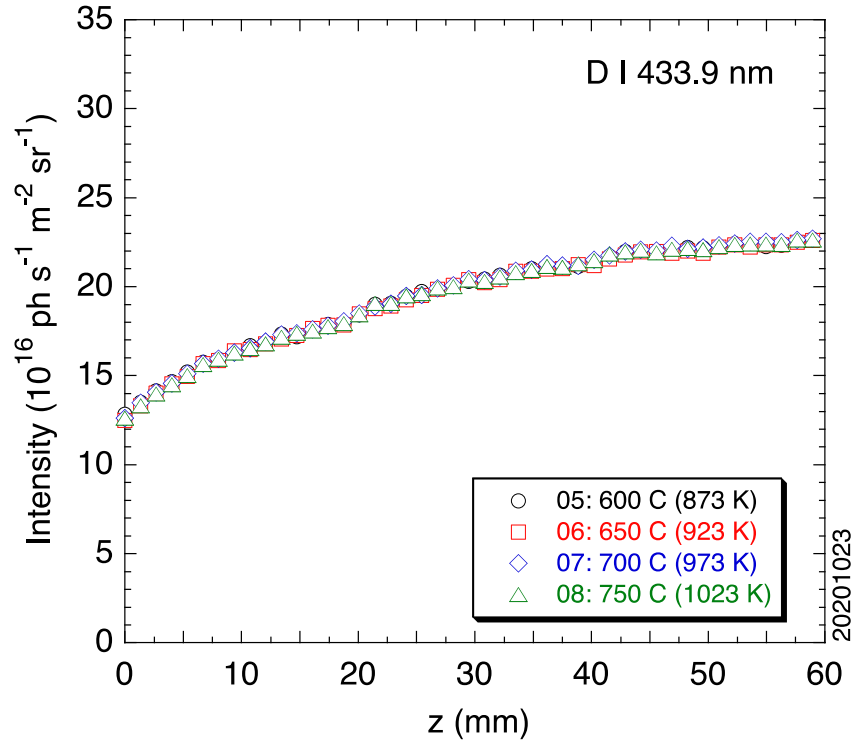

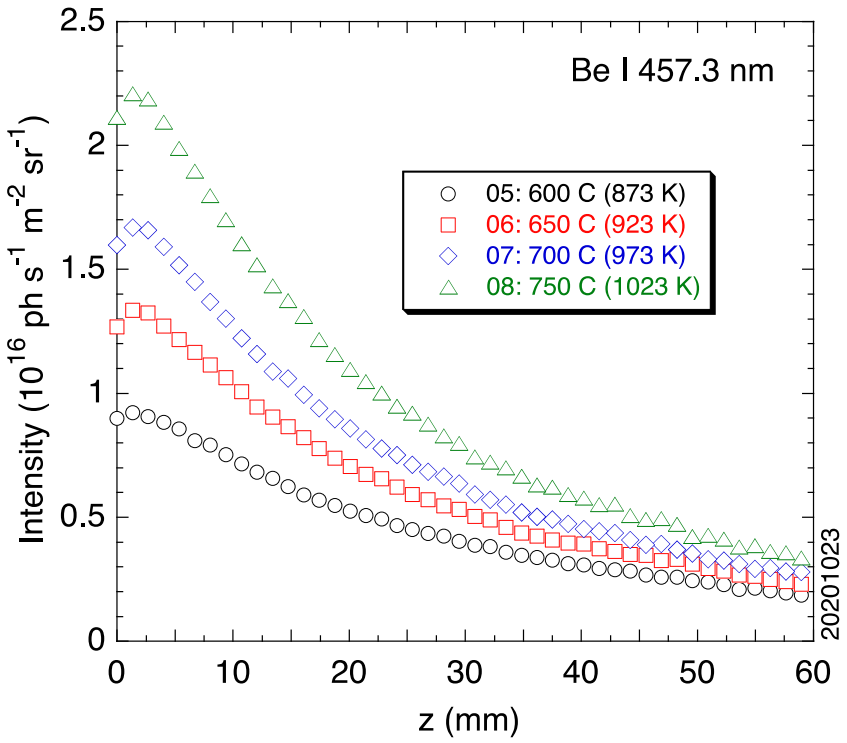

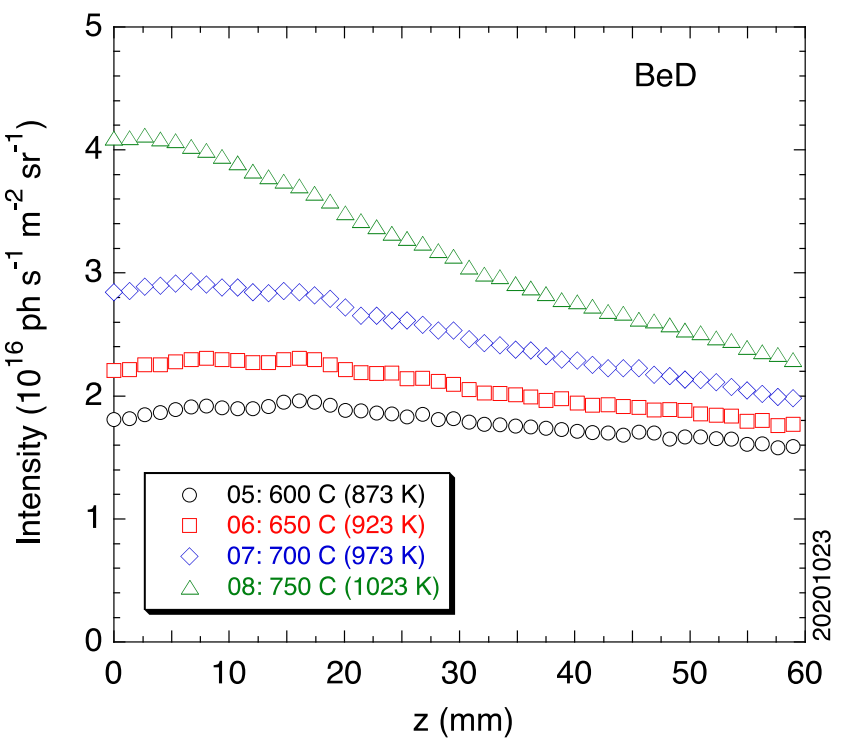

Specim IQ is also used to observe 2D emission profiles of a Be I line at 457.3 nm and a BeD A-X band.

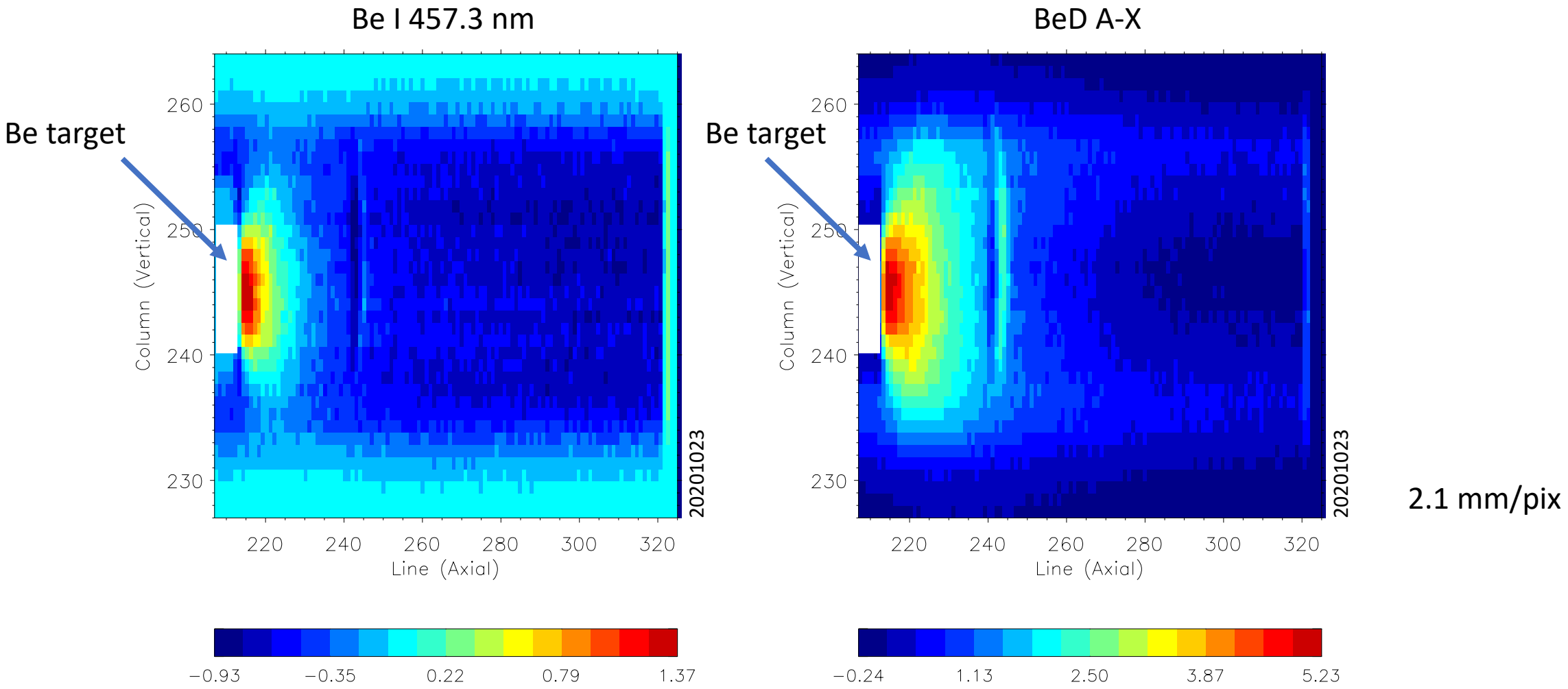

PISCES – future direction

PISCES-RF uses the liquid-cooled RF helicon source developed w/ ORNL for MPEX

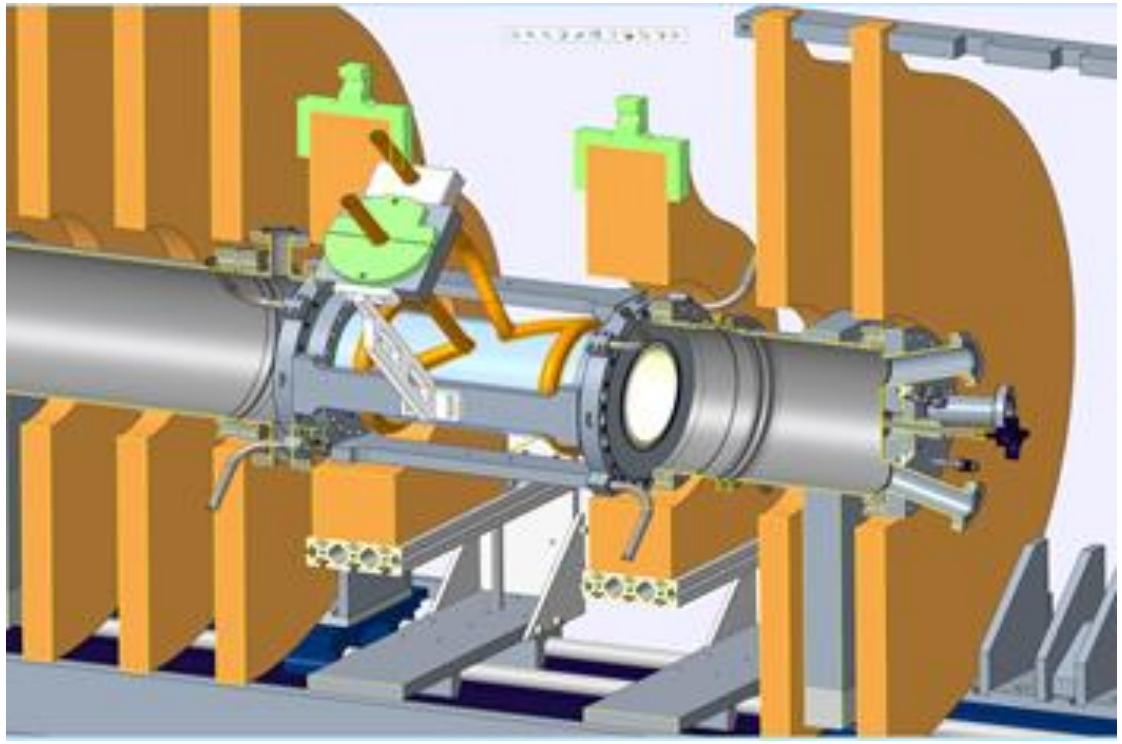

CAD model

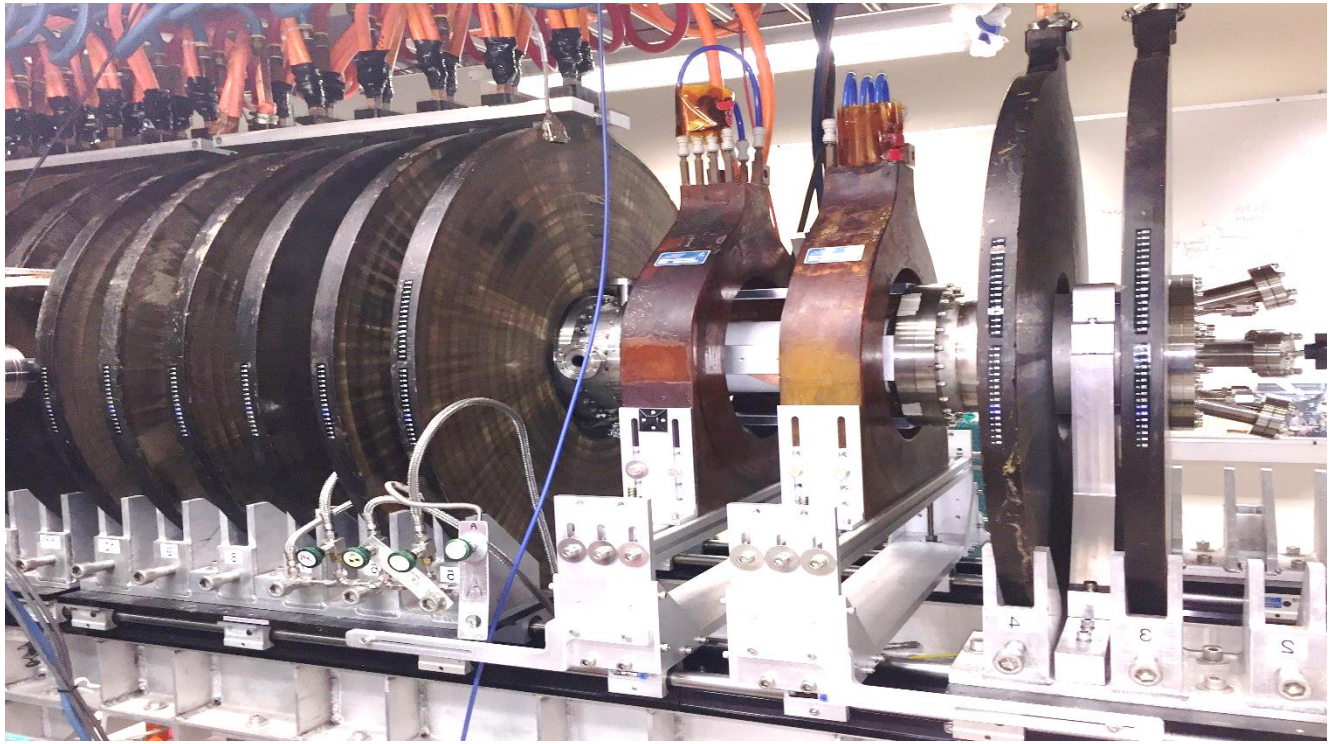

RF source assembly installed on UCSD-CSDX Device (before attaching the RF shielding)

PISCES-RF Source Has Produced High Flux Plasmas

Probe @ 0.8 m downstream from RF source

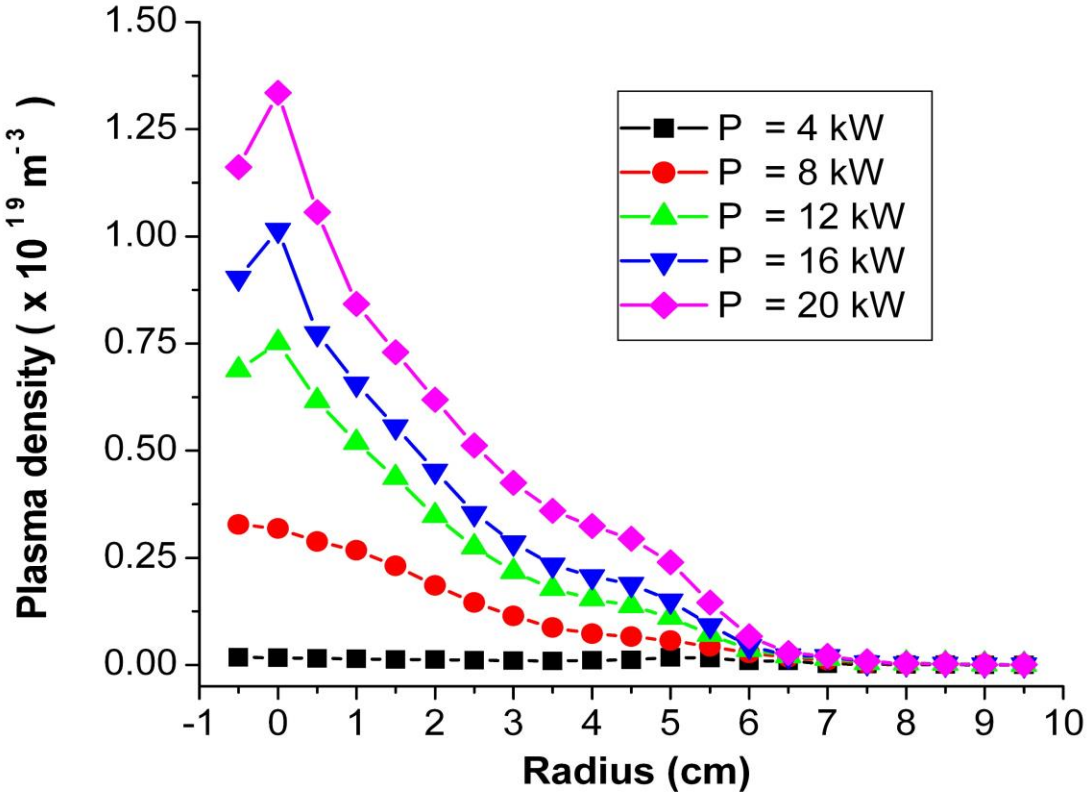

Electron temperature ~ 4 – 8 eV

Particle flux ~ 3 x 10^{23} $m^{-2}sec^{-1}$

Probe @ 1.5 m downstream from RF source

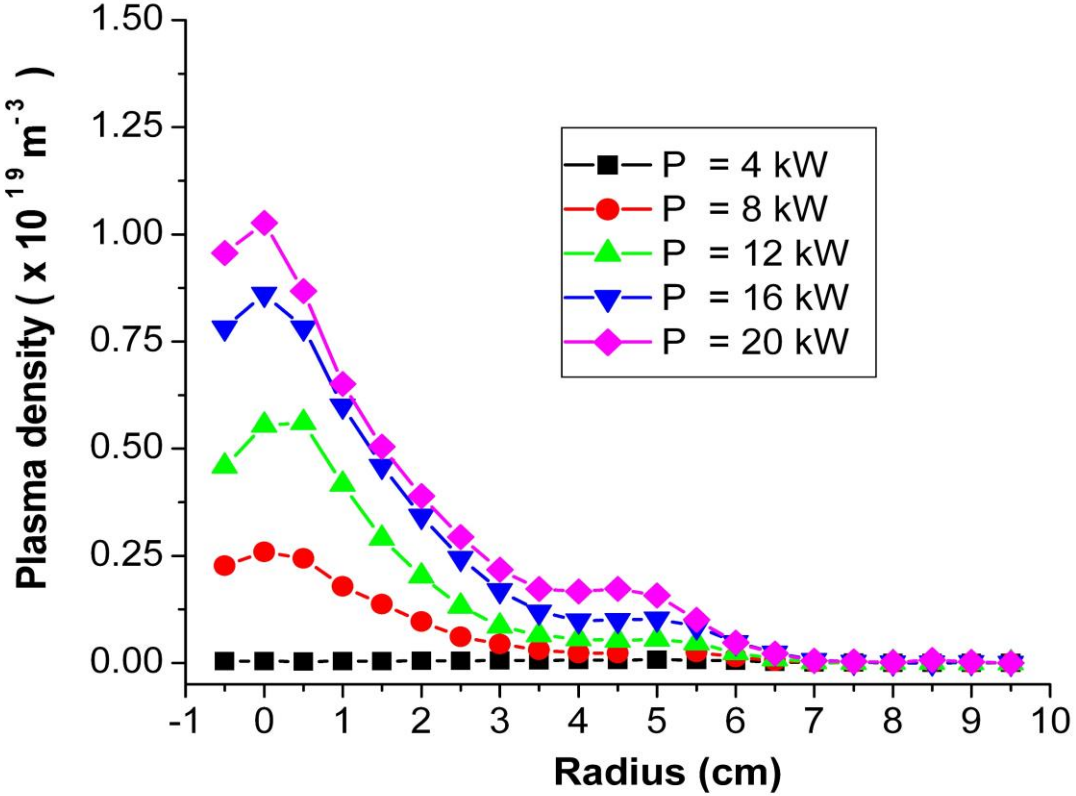

Electron temperature ~ 3 – 4 eV

Particle flux ~ 2 x 10^{23} $m^{-2}sec^{-1}$

S. C. Thakur *et. al.*, "PISCES-RF: a liquid-cooled high-power steady-state helicon plasma device" *submitted to* Plasma Sources Science and Technology (2020)

The PISCES-RF Concept for in-situ PMI Studies

Liquid cooled 30 kW MPEX rf helicon source

Chamber cooling added

Target - plasma exposure position

Target load-lock entry

Actively cooled target manipulator

In-line laser entry port

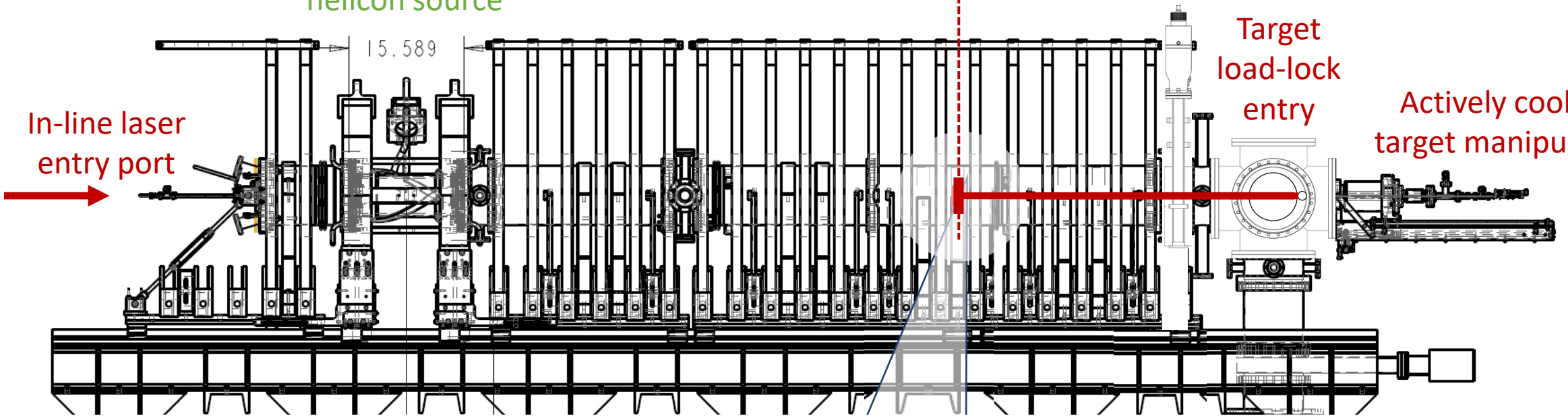

- Recent Upgrades are from ORNL Plasma Source development Supplement & A LIDS Measurement and Innovation Award: DE-SC001-8281

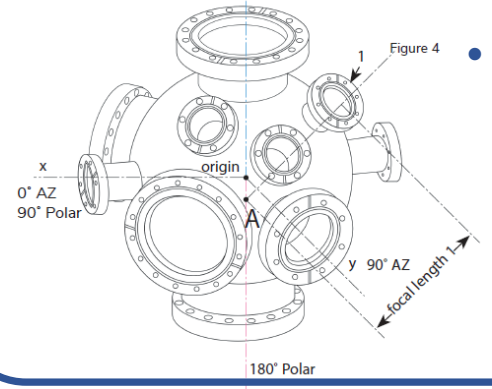

- Design and acquire a multi-port focused target exposure chamber to allow in-situ laser based and optical diagnostic capabilities LIBS, LIDS, TGS, & HIS